

# Absorption and dispersion in the O<sub>2</sub> microwave spectrum at atmospheric pressures

Earl W. Smith

National Bureau of Standards, Boulder, Colorado 80302  
(Received 8 January 1981; accepted 24 February 1981)

Calculations are performed for absorption and phase dispersion at various frequencies within the 60 GHz band of O<sub>2</sub> from low pressures where the spectral lines are isolated, to atmospheric pressures where they merge to form a continuum band. A perturbation theory proposed by Rosenkranz was tested and found to be valid for pressures up to 100 kPa (1 atm). The "line coupling coefficients", which describe the transfer of excitation from one radiating state to another, are also studied and various methods for evaluating these coefficients are analyzed and compared with experimental data. It is found that dispersion measurements are extremely sensitive to these coefficients and an experimental procedure for systematically measuring them is outlined; it is shown that such measurements can provide a very sensitive test for theoretical calculations of inelastic transition amplitudes.

## I. INTRODUCTION

The overlap of spectral lines at high pressures provides an interesting means for studying inelastic rates. To illustrate this we first note that the linewidth for a collision broadened spectral line is the sum of two terms, an elastic term due to collisions which reorient the radiating dipole, changing the azimuthal quantum number  $M$ , and an inelastic term due to collisions which transfer excitation out of the states involved in the radiative transition, e.g., Sec. V of Ref. 1. At high pressures, when the individual spectral lines merge to form a band, inelastic collisions which transfer excitation from one radiating state to another (called "line coupling transitions") are no longer effective in broadening since they only shift intensity from one part of the band to another; see Gordon,<sup>2</sup> p. 454. The half-width  $w$  of the band will thus be smaller than the half-widths of the isolated lines; the observed width  $Pw$  (in cm<sup>-1</sup> or MHz) will of course be larger simply because the pressure  $P$  is larger. These line coupling transitions will be studied in terms of their effect on absorption and dispersion (the frequency dependent part of the index of refraction). It will be shown that the dispersion is extremely sensitive to these inelastic transitions and that, in some cases, it permits a direct measurement of the inelastic rate coupling two radiating states. Such measurements could provide a useful addition to the usual measurements of decay rates, etc., since the latter are usually given by a sum of inelastic transitions whereas the former are often determined by a single state to state transition probability. Direct measurements of state to state transition rates can provide a very stringent test for theoretical calculations. Thus, a major goal of the present paper is to demonstrate this type of analysis by studying the inelastic transition rates recently calculated by Lam<sup>3,4</sup> for the 60 GHz band of O<sub>2</sub> and comparing them with experimental measurements performed on this band.<sup>5,6</sup>

In order to study the effect of inelastic transitions on absorption and dispersion, it is first necessary to have a line shape theory which is numerically accurate and, at the same time, analytically simple enough to permit a clear determination of the role of each inelastic rate. For a band composed of many spectral lines, the line

shape expression itself can pose serious problems. For example, the 60 GHz spectrum of O<sub>2</sub> studied in this paper requires the calculation of at least 44 spectral lines; thus, taking careful account of all line coupling terms, the line shape calculation requires inversion of a 44×44 matrix for each value of pressure and frequency of interest. Using a computer, this is expensive but not difficult; however, with such a numerical analysis, one loses sight of the effect of the individual inelastic rates. In an attempt to avoid this difficulty, Rosenkranz<sup>7</sup> has employed perturbation theory to derive a relatively simple line shape expression which provides physical insight into the effect of the inelastic rates and is numerically accurate for most calculations. A second major goal of the present paper is to make certain improvements in the Rosenkranz perturbation approach and to confirm the numerical accuracy of this approach by comparison with brute force numerical calculations employing a matrix inversion; specific calculations will be performed for the 60 GHz band of O<sub>2</sub>.

The absorption and dispersion of microwaves due to oxygen at atmospheric pressures are of interest in their own right for a variety of communications and remote sensing problems. Thus, there exist accurate absorption and dispersion measurements over a wide range of pressures, thereby making this microwave spectrum an attractive test case for microwave line broadening theories. It is hoped that the present analysis will help to clarify the interpretation of some of these experimental data.

## II. GENERAL THEORY

### A. Properties of the O<sub>2</sub> microwave spectrum

The microwave spectrum of O<sub>2</sub> is due to a series of magnetic dipole transitions within the <sup>3</sup>Σ<sub>g</sub> electronic ground state. The nuclear rotation  $N$  couples to the electronic spin  $S=1$  to produce a total angular momentum  $J$  which may take the values  $J=N, N±1$ . This triplet of rotational states is split by spin-spin and spin-orbit interactions, resulting in the energy level structure shown in Fig. 1. Within each triplet (labeled by  $N$ ) there are two allowed microwave transitions  $J=N→J=N+1$ , denoted by  $ν_N^+$ , and  $J=N→J=N-1$ , denoted by  $ν_N^-$ .

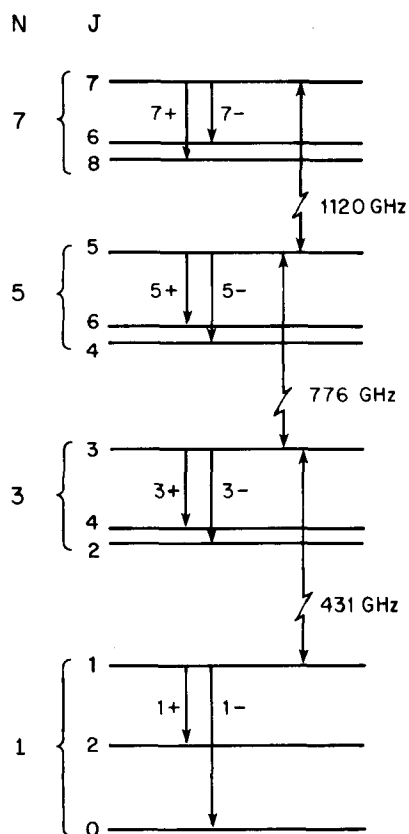


FIG. 1. Rough energy level diagram showing the multiplet structure of O<sub>2</sub>. The resonant magnetic dipole transitions are denoted by  $N^{\pm}$  (the  $1^-$  line at 118 GHz is somewhat separated from the rest of the band). For  $N \leq 5$ , the state  $J=N-1$  has a lower energy than  $J=N+1$  and for  $N > 5$  the converse is true.

These transitions, referred to as the "resonant transitions," lie in the range 50–70 GHz except for  $\nu_1^{\pm} = 119$  GHz; a list of transition frequencies and line strengths is given in Table I (obtained from Ref. 8).

There are also some magnetic dipole transitions  $J=N+1 \rightarrow J=N+1$ ,  $J=N-1 \rightarrow J=N-1$ , and  $J=N \rightarrow J=N$  (referred to as  $0_N^+$ ,  $0_N^-$ , and  $0_N$ , respectively) which occur at zero frequency and are usually called "non-resonant transitions." At atmospheric pressures these nonresonant lines make a small contribution (1%–10%) to the absorption and dispersion in the 60 GHz region; hence, they will be included in our analysis. The  $\nu_N^+$  and  $\nu_N^-$  lines are occasionally referred to simply as  $N^+$  and  $N^-$  lines in cases where there can be no confusion with the  $0_N^+$  and  $0_N^-$  lines.

The resonant transitions produce a series of isolated Lorentzian spectral lines whose widths have been measured and compared with theoretical calculations many times. The most recent work<sup>3,6,9</sup> has produced very satisfactory agreement between theory and experiment so that one feels confident that these linewidths are known accurately to within about 5% (theoretical uncertainties may be slightly larger due to the lack of an accurate potential surface).

There are four pairs of lines ( $3^-$ ,  $13^+$ ), ( $7^+$ ,  $5^-$ ), ( $3^+$ ,  $9^-$ ), and ( $15^-$ ,  $1^+$ ) that have a frequency spacing which is

about 1/5 of the normal separation between lines (see Table I). These doublets merge at pressures around 5 kPa (0.05 atm) and all lines begin to merge with their neighbors at pressures around 30 kPa (0.3 atm), finally producing an unstructured absorption band at 100 kPa (1 atm). This band extends from 50 to 70 GHz with a collision broadened line, the  $\nu_1^-$  line, at 120 GHz (see Fig. 2). At pressures above 0.1 atm it is no longer possible to describe the spectrum as a simple superposition of overlapping but noninterfering Lorentzian lines because the line coupling transitions have already begun to produce observable effects (discussed in detail in Sec. III).

### B. The line shape expression and notation

In this paper we will use the impact theory<sup>10</sup> to describe the collision broadening of the spectrum. The impact theory assumes that (1) the radiating or absorbing molecule is perturbed by a sequence of binary collisions with other particles and (2) the duration of these collisions is short enough that, if a collision occurs, it can be completed during all times of interest for spectral line broadening. For broad absorption bands at high pressures, it is worth reviewing the validity of these assumptions. The assumption of binary collisions will break down at high pressures when the particle density  $n$  becomes comparable with the "interaction volume"  $\pi b^3$ , where  $b$  is the "range" of the interaction, e.g., for a Lennard-Jones 6-12 potential,  $b$  would be the order of the internuclear distance at the point of maximum attractive interaction. For strong interactions between permanent dipoles,  $b$  may be somewhat larger than the position of the attractive well; hence, the validity of the binary collision approximation should be reconsidered for pressures above 1 MPa (10 atm). There is no problem with the present work since the highest pressure considered is 100 kPa (1 atm). The second assumption, often called the completed collision assumption,<sup>1</sup> means that all collisions will be described

TABLE I. Partial list of spectral lines and their frequencies; a more complete list is given in Table I of Ref. 8.

Line	(GHz)	
17 <sup>+</sup>	63.5685	
15 <sup>+</sup>	62.9980	
3 <sup>-</sup>	62.4863	} Doublet
13 <sup>+</sup>	62.4112	
11 <sup>+</sup>	61.8002	
9 <sup>+</sup>	61.1506	
7 <sup>+</sup>	60.4348	} Doublet
5 <sup>-</sup>	60.3061	
5 <sup>+</sup>	59.5910	
7 <sup>-</sup>	59.1642	
3 <sup>+</sup>	58.4466	} Doublet
9 <sup>-</sup>	58.3239	
11 <sup>-</sup>	57.6125	
13 <sup>-</sup>	56.9682	
15 <sup>-</sup>	56.3634	} Doublet
1 <sup>+</sup>	56.2648	
17 <sup>-</sup>	55.7838	

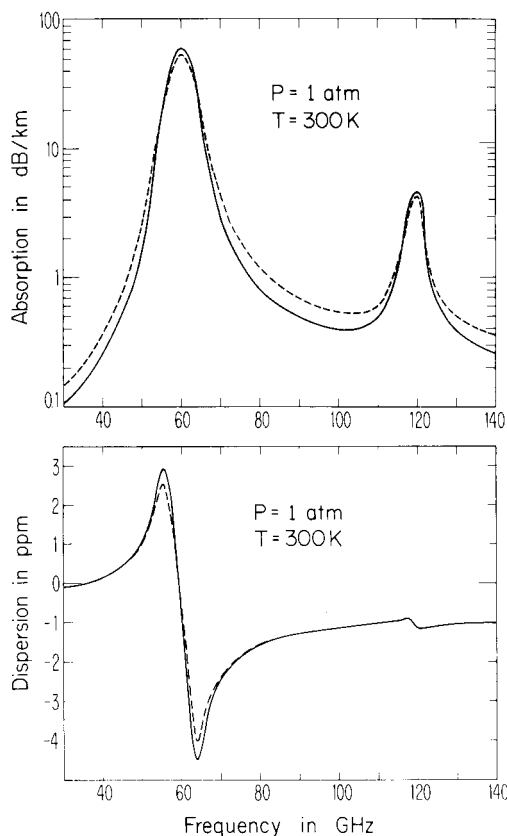


FIG. 2. Absorption and dispersion as a function of frequency, illustrating the difference between a pure Van Vleck-Weisskopf (VW) calculation (dashed curve) and a calculation which accounts for line coupling effects (solid curve). Throughout this paper, a VW calculation refers to a simple superposition of Lorentzian lines whose linewidths (Table II) are determined by low pressure measurements; this sum of Lorentzian lines includes the "resonant lines" at the frequencies  $\nu_j > 0$ , "nonresonant lines" for which  $\nu_j = 0$ , and "negative resonant lines" for which  $\nu_j < 0$  (discussed in Sec. II B).

by an  $S$  matrix which represents the effect of a complete collision. To show that this assumption limits the impact theory to the line center, we recall that the intensity  $I(\nu)$  (for either emission or absorption) at a frequency separation  $\Delta\nu = (\nu - \nu_0)$  from the line center  $\nu_0$  is given by the Fourier transform of a dipole correlation function<sup>3,10</sup>  $C(t) = \langle d(t)d(0) \rangle$ :

$$I(\nu) \propto \int_0^{\infty} C(t) \exp(2\pi i \Delta\nu t) dt. \quad (1)$$

Since the exponential oscillates rapidly for large values of  $t$ , the integral is determined mainly by  $t \lesssim 1/(2\pi\Delta\nu)$ . If the average duration of a collision is  $\tau$ , then there will be a region in the line wings  $\Delta\nu > 1/(2\pi\tau)$  where the intensity is determined entirely by times  $t < \tau$ , which are so short that most collisions cannot be regarded as completed and the  $S$  matrix does not adequately describe their effect. For O<sub>2</sub> at 300 K,  $\tau \approx 5 \times 10^{-13}$  s; hence, the impact theory can be used for  $\Delta\nu < 300$  GHz, which is quite adequate for all  $\Delta\nu$  of interest for the 60 GHz band. However, for some infrared bands such as those of HCl, the line spacing is on the order of  $1/(2\pi\tau)$  and nonimpact effects have been seen between the spectral

lines<sup>11</sup>; one should therefore be aware of the possibility of encountering nonimpact effects in very broad molecular bands.

Within the framework of the impact theory, the expressions for the absorption coefficient  $k(\nu)$  and the index of refraction  $n(\nu)$  are given by<sup>12</sup>

$$k(\nu) = -\frac{2(2\pi\nu)^2 N}{3ckT} \text{Im} I(\nu), \quad (2)$$

$$\begin{aligned} n(\nu) - 1 &= -\frac{2(2\pi\nu)^2 N}{3ckT} \text{Re} I(\nu) \\ &= \frac{2(2\pi\nu)^2 N}{3ckT} \Delta N(\nu), \end{aligned} \quad (3)$$

where  $\Delta N(\nu) \equiv -\text{Re} I(\nu)$  is called the phase dispersion<sup>8</sup> and the complex line shape function  $I(\nu)$  is given by

$$I(\nu) = \sum_{jk} d_j \langle j | [(\nu - \nu_0) - iP\nu]^{-1} | k \rangle d_k \rho_k. \quad (4)$$

In Eq. (4),  $|j\rangle$  and  $|k\rangle$  denote "doubled state vectors" which are given in terms of ordinary O<sub>2</sub> states  $|NSJM\rangle$  and the Wigner  $3j$  symbol [e.g., Eqs. (18) and (19) of Ref. 13]

$$\begin{aligned} |NSJ, N'SJ', KQ\rangle &= \sqrt{2K+1} \sum_{MM'} (-1)^{J'+M'+K} \\ &\times \begin{pmatrix} J & J' & K \\ -M & M' & Q \end{pmatrix} |NSJM\rangle \langle N'SJ'M'|. \end{aligned} \quad (5)$$

The  $d_j$  in Eq. (4) denote the reduced matrix elements [e.g., Eqs. (21) and (22) of Ref. 13]

$$\begin{aligned} \langle NSJ || d || N'SJ' \rangle &\equiv \sqrt{3} \sum_{MM'} (-1)^{J-M} \\ &\times \begin{pmatrix} J' & 1 & J \\ -M' & q & M \end{pmatrix} \langle NSJM | d_q | N'SJ'M' \rangle, \end{aligned} \quad (6)$$

where the  $d_q$  are the components of the magnetic dipole moment  $\mathbf{d}$  and  $\rho_k$  denote the density matrix elements (statistical weights) which are well approximated by<sup>14</sup>

$$\begin{aligned} \langle NSJ || \rho || N'SJ' \rangle &\approx \delta_{BB'} \delta_{JJ'} \rho(N) \\ &\approx \delta_{NN'} \delta_{JJ'} \frac{\exp(-E_N/kT)}{0.725 kT}, \end{aligned} \quad (7)$$

where  $E_N/k = 2.0685 N(N+1)$  is the energy of the  $N$ th multiplet in  $K$ . The frequency  $\nu$  in Eq. (4) is diagonal,  $\langle j | \nu | k \rangle = \nu_j \delta_{jk}$ , and  $\nu_0$  is also a diagonal matrix  $\langle j | \nu_0 | k \rangle = \nu_j \delta_{jk}$ , where  $\nu_j$  is the energy difference (divided by  $h$  so as to give a frequency) between the two states  $NJ$  and  $N'J'$  which are combined to form the doubled state  $|j\rangle$  [cf. Eq. (5)]. Notice that the only states  $|j\rangle$  and  $|k\rangle$  required by Eq. (4) are those which correspond to allowed dipole transitions (i.e., those for which  $d_j$  and  $d_k$  are nonzero); hence, the only frequencies  $\nu_j$  which appear are those corresponding to allowed spectral lines. Consequently, the vectors  $|j\rangle$  and  $|k\rangle$  are often referred to as states in "line space." The matrix  $\langle j | w | k \rangle$ , whose form will be given in Sec. III, therefore represents the coupling between the spectral lines

$j$  and  $k$  which was discussed above; the diagonal elements  $w_{jj}$  give the linewidth and shift for the spectral line  $j$ .

In our calculations of the O<sub>2</sub> microwave spectrum we have included three groups of spectral lines. The first group contains the 44 resonant transitions  $\nu_N^*$  for  $N \leq 43$ , the second group contains the 44 nonresonant lines at  $\nu = 0$  denoted by  $0_N^*$ , and the third group contains 44 "negative resonance lines" which act like a group of spectral lines located at negative frequencies  $-\nu_N^*$ . The negative resonance lines occur because the line profile is given by a Fourier transform [Eq. (1)] which contains terms like  $\exp[i(\nu - \nu_j)t]$  as well as  $\exp[i(\nu + \nu_j)t]$ ; the former give rise to the normal resonant transitions  $\langle j | \nu_0 | j \rangle = \nu_j > 0$  in Eq. (4), and the latter produce the negative resonance lines  $\langle j | \nu_0 | j \rangle = \nu_j < 0$  in Eq. (4), which contribute to  $I(\nu)$  as though they were spectral lines located at negative frequencies. Since the bandwidth is the order of 20 GHz, these three groups of spectral lines are well separated from one another; hence, the nonresonant lines and the negative resonance lines contribute to the observed band at 60 GHz only by means of their far line wings. This contribution is usually on the order of 1% or less; however, when the dispersion due to  $\nu_N^*$  lines is very small, namely, near band center (see Fig. 2), the contribution from the  $0_N^*$  and  $-\nu_N^*$  lines can be quite important (see the discussion of the 5\* dispersion in Sec. III. D).

Since these three groups of lines are well separated from one another, it is possible to neglect any line coupling between groups (recall the discussion of the importance of line coupling terms in Sec. I). This has been verified by numerical calculations which show that line coupling to either the  $0_N^*$  or  $\nu_N^*$  produces changes smaller than 0.001%. Neglecting line coupling between the three groups of lines makes the matrix  $(\nu - \nu_0) - iPw$  in Eq. (4) block diagonal and each of the three blocks, corresponding to the groups  $\nu_N^*$ ,  $0_N^*$ , and  $-\nu_N^*$ , is then a  $44 \times 44$  matrix. The matrix inversion is thus greatly simplified but still very time consuming, being more than 100 times slower than the perturbation calculation discussed in the following section.

We mention in passing that the group of nonresonant lines  $0_N$  corresponding to  $J=N \rightarrow J=N$  transitions has not been included because its transition dipole strengths are an order of magnitude smaller than those for the  $0_N^*$  transitions (Lam<sup>4</sup>, p. 104).

### C. Perturbation theory

Rosenkranz<sup>7</sup> has developed a perturbation theory approach to the matrix inversion in Eq. (4) which provides a very useful physical insight into the role played by the line coupling coefficients  $w_{jk}$ . His work is an expanded quantum mechanical version of an earlier classical theory by Gordon<sup>2</sup> and, as such, it retains much of the physical insight and numerical simplicity of the latter while improving on mathematical rigor and quantitative accuracy. Unfortunately, the Rosenkranz theory also contains some notational differences from the mainstream of quantum mechanical line broadening theories (Baranger,<sup>10</sup> Ben-Reuven,<sup>13</sup> and Lam<sup>3</sup>), as well as re-

taining some classical approximations which can be improved upon. In this section we will extend the perturbation approach using the more common quantum mechanical notation and will avoid some of the classical approximations retained by Rosenkranz.

The main notational differences from Rosenkranz theory are found by comparing our  $d_k$  and  $\rho_k$  [Eqs. (6) and (7), respectively] with Rosenkranz [Eqs. (4)–(7)]. Our  $d_k$  are reduced matrix elements of the dipole operator [see Lam,<sup>3</sup> Eqs. (65)–(70)] which are proportional to the Rosenkranz  $d_N^*$  multiplied by  $\sqrt{2N+1}$  and our  $\rho_k$  are reduced matrix elements of the density matrix which are equal to his  $\Phi_N$  divided by  $(2N+1)$ . Our matrix  $w_{jk}$  will therefore equal his  $w_{NN}$  multiplied by  $\sqrt{(2N'+1)/(2N+1)}$ .

As noted above, the basic idea behind the Rosenkranz approach is to invert the matrix  $(\nu - \nu_0) - iPw$  by using perturbation theory. Specifically, one expresses the eigenvalues and eigenvectors of the matrix  $\nu_0 + iPw$  by a perturbation expansion in powers of  $Pw_{jk}/\nu_{jk}$ , where  $\nu_{jk} = \nu_j - \nu_k$  is the difference between the frequencies of two different spectral lines. It is then possible to diagonalize the matrix  $\nu_0 + iPw$  by means of a transformation  $X^{-1}(\nu_0 + iPw)X$  so that

$$\langle j | (\nu - \nu_0 - iPw)^{-1} | k \rangle = \sum_l X_{jl} (\nu - \Lambda_l)^{-1} (X^{-1})_{lk}, \quad (8)$$

where  $\Lambda_l$  are the eigenvalues of  $\nu_0 + iPw$  and  $X_{lk}$  is a matrix whose columns are the normalized eigenvectors. The line shape [Eq. (4)] is then given by

$$I(\nu) = \sum_{jk} d_j (X_{jl}) (\nu - \Lambda_l)^{-1} (X^{-1})_{lk} d_k \rho_k, \quad (9)$$

which is quite easy to evaluate since it does not involve a matrix inversion.

The validity of this approach requires that  $Pw_{jk}/\nu_{jk}$  be small for all lines  $j$  and  $k$ . The size of these terms will be discussed further in Sec. III but for the moment we note that there is an immediate problem because  $\nu_j = 0$  for all of the nonresonant lines; hence,  $w_{jk}/\nu_{jk}$  will diverge when both  $j$  and  $k$  are nonresonant lines. Rosenkranz used an idea from Gordon's classical theory to merge all nonresonant lines into one and to replace the coupling to this nonresonant line by a classical expression [Ref. 7, Eq. (10)]. While this approximation is not at all serious (the nonresonant lines produce at most a 10% effect), it is also unnecessary if one makes a minor change in the mathematical procedure. Our perturbation expansion is derived in the Appendix and the results are summarized in Eqs. (A17)–(A21), where  $\sum_{j \neq k}$  is to be interpreted such that, whenever  $k$  corresponds to a nonresonant line  $\nu_k = 0$ , the sum over  $j$  includes only the resonant lines  $\nu_j > 0$  and the "negative resonant" lines  $\nu_j < 0$ . A comparison with Rosenkranz perturbation theory (the Appendix of Ref. 7) shows that, except for the treatment of the nonresonant lines, the two approaches are identical to first order in  $P$ ; we have also evaluated the second order terms to permit a test of the perturbation method (i. e., the second order terms should produce only a small correction).

We now substitute Eq. (9) into Eq. (4) to obtain

$$\text{Im } I(\nu) = \sum_i \frac{\text{Im}(\Lambda_i) \text{Re}(G_{ii}) + [-\text{Re}(\Lambda_i)] \text{Im}(G_{ii})}{[\nu - \text{Re}(\Lambda_i)]^2 + \text{Im}(\Lambda_i)^2} \quad (10)$$

and

$$\begin{aligned} G_{ii} &\equiv \sum_{jk} (X^{-1})_{ik} \rho_k d_k d_j X_{ji} \\ &= \rho_i d_i^2 - iP d_i \sum_{j \neq i} d_j (w_{ji} \rho_i + w_{ij} \rho_j) / \nu_{ji} + P^2 \rho_i d_i^2 \sum_{j \neq i} w_{ij} w_{ji} / \nu_{ji}^2 + P^2 d_i \sum_{j \neq i} d_j (w_{ji} \rho_i + w_{ij} \rho_j) w_{ij} / \nu_{ji}^2 \\ &\quad - P^2 d_i \sum_{j \neq i} \sum_{k \neq i} d_j (w_{jk} w_{ki} \rho_i + w_{ik} w_{kj} \rho_j) / \nu_{jk} \nu_{ik} - P^2 \sum_{j \neq i} (d_j w_{ji} / \nu_{ji}) \sum_{k \neq i} (d_k w_{ik} \rho_k / \nu_{ki}) + \dots \end{aligned} \quad (12)$$

Equation (10) is identical to Rosenkranz [Eq. (A2)] and his  $G_{kk}$  in Eq. (A6) agrees with our Eq. (12) to first order in  $P$ . Next using [Ben-Reuven,<sup>13</sup> Eq. (41)]

$$w_{jk} \rho_k = w_{kj} \rho_j, \quad (13)$$

Eq. (12) becomes

$$G_{kk} = \rho_k d_k^2 (1 + iP y_k + P^2 g_k), \quad (14)$$

$$y_k = 2 \sum_{j \neq k} (d_j / d_k) w_{jk} / \nu_{kj}, \quad (15)$$

$$\begin{aligned} g_k &= \sum_{j \neq k} w_{kj} w_{jk} / \nu_{jk}^2 - \left[ \sum_{j \neq k} (d_j / d_k) w_{jk} / \nu_{jk} \right]^2 \\ &\quad + 2 \sum_{j \neq k} (d_j / d_k) w_{jk} w_{kk} / \nu_{jk}^2 - 2 \sum_{j \neq k} (d_j / d_k) w_{ji} w_{ik} / \nu_{jk} \nu_{ik}. \end{aligned} \quad (16)$$

Using these expressions, Eqs. (10) and (11) become

$$\begin{aligned} \text{Im } I(\nu) &= P \sum_k \rho_k d_k^2 \left[ \frac{w_{kk} (1 + P^2 g_k) + (\nu - \nu_k + P^2 \delta \nu_k) y_k}{(\nu - \nu_k + P^2 \delta \nu_k)^2 + (P w_{kk})^2} \right] \\ &= P \sum_k \rho_k d_k^2 \left[ \frac{w_{kk} + (\nu - \nu_k) y_k}{(\nu - \nu_k)^2 + (P w_{kk})^2} \right] \quad (\text{first order}), \end{aligned} \quad (17)$$

$$\begin{aligned} \text{Re } I(\nu) &= \sum_k \rho_k d_k^2 \left[ \frac{(\nu - \nu_k + P^2 \delta \nu_k) (1 + P^2 g_k) + (P w_{kk}) (P y_k)}{(\nu - \nu_k + P^2 \delta \nu_k)^2 + (P w_{kk})^2} \right] \\ &= \sum_k \rho_k d_k^2 \left[ \frac{(\nu - \nu_k) + (P w_{kk}) (P y_k)}{(\nu - \nu_k)^2 + (P w_{kk})^2} \right] \quad (\text{first order}), \end{aligned} \quad (18)$$

where  $\delta \nu_k$  is a second order shift defined by

$$\delta \nu_k = \sum_{j \neq k} w_{kj} w_{jk} / \nu_{jk}. \quad (19)$$

In deriving Eqs. (17) and (18) we have assumed that  $w_{kk}$  is real, thereby neglecting any first order pressure shifts. This is consistent with experimental observations at low pressures.<sup>5</sup> At high pressures it is not

$$\text{Re } I(\nu) = \sum_i \frac{\text{Re}(\nu - \Lambda_i) \text{Re}(G_{ii}) - \text{Im}(\Lambda_i) \text{Im}(G_{ii})}{[\nu - \text{Re}(\Lambda_i)]^2 + \text{Im}(\Lambda_i)^2}, \quad (11)$$

where, using Eqs. (A20), (A21), and some straightforward but tedious algebra,

possible to measure a pressure shift since all lines overlap; nonetheless, it is safe to neglect any linear pressure shift since it would have been detected at the lower pressures (line center frequencies can be measured with very high accuracy at low pressures<sup>8</sup>). Our theory contains a quadratic pressure shift  $\delta \nu_k$  which cannot be ruled out on the basis of low pressure measurements; hence, it will be retained. Comparing Eq. (17) with Rosenkranz [Eq. (2)] it is clear that our formal results are identical to first order in pressure; our Eq. (17) also contains two second order contributions  $g_{kk}$  and  $\delta \nu_k$ . We must emphasize, however, that our matrices  $d_k$ ,  $\rho_k$ , and  $w_{kj}$  differ from those used by Rosenkranz by the factors  $(2N+1)$  discussed earlier.

#### D. Line coupling coefficients—Rosenkranz prescription

When Rosenkranz developed his theory for the O<sub>2</sub> microwave spectrum, there were no calculations of line coupling coefficients  $w_{jk}$  available and even the half-widths were only known to within an order of magnitude. He therefore adopted an approximate prescription for evaluating  $w_{jk}$  which provides order of magnitude accuracy. However, as more accurate measurements became available,<sup>5</sup> attempts to fit the growing body of experimental data by using the Rosenkranz prescription for the  $w_{jk}$  began to produce results that were inconsistent.

The central equation in the Rosenkranz prescription for calculating  $w_{jk}$  is  $\sum_j w_{jk} = 0$  [Ref. 7, Eq. (14)]. This result is obtained by assuming that  $w_{jk}$  is proportional to a cross section [Ref. 7, Eq. (8)] which would result in this conservation of probability summation rule. Although one often speaks of an "optical cross section," it should be emphasized that this is not a true cross section in the usual probabilistic sense. The actual quantum mechanical expression for  $w_{jk}$  is obtained from Lam<sup>3</sup> [Eqs. (30), (34), (51), and (48)] in the form

$$\begin{aligned} ((N_a J_a, N_b J_b | w | N'_a J'_a, N'_b J'_b)) &= \sum_{M_a M'_a M_b M'_b} (-1)^{J_a + J'_a - M_a - M'_a} \begin{pmatrix} J_a & 1 & J'_a \\ -M_a & Q & M'_a \end{pmatrix} \begin{pmatrix} J_b & 1 & J'_b \\ -M_b & Q & M'_b \end{pmatrix} \\ &\quad \times [\delta_{J_a J'_a} \delta_{J_b J'_b} \delta_{M_a M'_a} \delta_{M_b M'_b} - (\langle N_a J_a M_a | S | N'_a J'_a M'_a \rangle \langle N_b J_b M_b | S | N'_b J'_b M'_b \rangle)_A \nu], \end{aligned} \quad (19)$$

where  $j$  represents the line  $N_a J_a \rightarrow N_b J_b$ ,  $k$  represents the line  $N_{a'} J_{a'} \rightarrow N_{b'} J_{b'}$ ,  $\{\dots\}_{AV}$  denotes an average over perturbers, and  $|N_a J_a M_a\rangle$  and  $|N_b J_b M_b\rangle$  are the initial states for the collisional transitions described by the  $S$  matrices. In a semiclassical formulation [e.g., Lam,<sup>3</sup> Eqs. (26)–(28)],  $\{\dots\}_{AV}$  is an average over impact parameters and velocities. Equation (19) is similar to, but not equal to, an inelastic transition rate and in particular it does not satisfy  $\sum_i w_{ik} = 0$ . By detailed numerical calculations with Lam's<sup>3</sup>  $w_{jk}$  we find that the sum of off diagonal  $w_{jk}$  is an order of magnitude smaller than  $w_{kk}$ ; thus, one may expect Rosenkranz's prescription to be accurate only to within an order of magnitude. In fact, Rosenkranz's  $w_{jk}$  are all within an order of magnitude of those calculated by Lam with most being a factor of 2 or 3 off. Liebe *et al.*<sup>5,8</sup> also used the Rosenkranz prescription together with a set of measured half-widths and again the calculated line coupling coefficients differed by factors of 2 or 3 from Lam's calculations and in addition the spectrum was extremely sensitive to the nonresonant linewidth, producing a value smaller than 1/2 of the value calculated by Lam.

### E. Line coupling coefficients—Lam's calculations

Lam<sup>3</sup> has employed a semiclassical theory developed by Dillon<sup>5</sup> to calculate linewidths and line coupling coefficients. His calculated linewidths agree closely with the measurements by Liebe *et al.*<sup>8</sup> and with independent calculations using a slightly different type of semiclassical theory.<sup>9</sup> While this agreement for half-widths gives some confidence in the accuracy of the theory, it is nonetheless clear that Lam has employed two approximations which are not valid for transitions between the multiplets, i.e.,  $\Delta N \neq 0$  transitions. These are (1) the infinite order sudden approximation for the  $S$  matrix and (2) the assumption that the target molecule can make an upward inelastic transition without taking energy from the translational motion. It will therefore be necessary to modify his  $w_{jk}$  in order to correct these approximations.

To infinite order sudden approximation assumes that one may neglect the exponential factors  $\exp(i\omega_{ab}t)$  which appear in the phase integrals

$$\eta_{ab} = \int_{-\infty}^{\infty} \exp(i\omega_{ab}t) V_{ab}(t) dt \quad (20)$$

that govern the  $S$  matrix  $S = \exp(-i\eta)$  [see Lam,<sup>3</sup> Eqs. (54) and (57)]. The argument for this approximation is that, with the collision centered at  $t=0$ , the interaction  $V(t)$  vanishes when  $t > \tau$ , where  $\tau$  denotes the collision duration time; hence,  $\exp(i\omega_{ab}t) \cong 1$  if  $\omega_{ab}\tau < 1$ , where  $\omega_{ab}$  is  $2\pi$  times the energy difference (in frequency units) between the states  $a$  and  $b$ . This approximation has been studied in great detail (e.g., Goldflam *et al.*)<sup>16</sup> and it is known to produce inelastic rates and half-widths which are too large when  $\omega_{ab}\tau \gtrsim 1$ . For O<sub>2</sub>, the average collision duration is  $\tau \cong 5 \times 10^{-13}$  sec and the frequency differences  $\omega_{ab}$  range from  $2\pi \times 431$  GHz  $\cong 2.7 \times 10^{12}$  s<sup>-1</sup> for  $N=1 \rightarrow N=3$  to  $2\pi \times 2155$  GHz  $\cong 1.4 \times 10^{13}$  s<sup>-1</sup> for  $N=11 \rightarrow N=13$ . Thus, we see that this approximation is not well satisfied for any of the  $\Delta N \neq 0$  transitions and it breaks down rather badly for larger  $N$ . This was not a

serious problem for Lam's half-width calculations since half-widths are determined by diagonal  $S$  matrix elements which are strongly affected by diagonal phase shift matrix elements  $\eta_{aa}$  for which  $\omega_{aa}=0$ ; nonetheless, the problem was observable even there (see Sec. III. A of Ref. 9). For inelastic processes involving off diagonal  $S$  matrix elements it is much more serious, producing errors on the order of a factor of 2 or 3. We have therefore used a crude semiempirical correction for this effect,<sup>17</sup> multiplying Lam's line coupling rates  $w_{jk}$  by  $\exp[-(6\pi^2 E_{jk} r_m / \alpha \bar{v})^{2/3} + (\epsilon + 0.5 E_{jk}) / kT]$ , where  $r_m = 3.67$  Å,  $\alpha = 19$ , and  $\epsilon = 156$  cm<sup>-1</sup> are the exponential -6 potential parameters for the O<sub>2</sub>-O<sub>2</sub> interaction,  $\bar{v}$  is the average velocity which is  $6.25 \times 10^4$  cm/s<sup>-1</sup> at 300 K,  $E_{jk}$  is the energy spacing  $B_e [N_j(N_j - 1) - N_k(N_k - 1)]$  between the rotational levels  $N_j$  and  $N_k$ , and  $B_e = 43.1$  GHz or  $1.44$  cm<sup>-1</sup>.

Lam's other main approximation is the assumption that the molecules can make inelastic transitions without any effect on their translational energy. This cannot be rigorously true since conservation of energy demands that any increase or decrease in rotational energy be balanced by a corresponding decrease or increase in translational kinetic energy. However, this approximation, very common in semiclassical line broadening theories, is justified if the inelastic transitions involve energy changes  $\Delta E_{ab}$  which are small compared with  $kT$ . The argument is that small changes in translational energy cause small changes in the trajectory which produce small changes in the phase integrals  $\eta_{ab}$  [Eq. (20)] whose effect on the  $S$  matrix can be shown to be negligible. Of course, there will always be some small translational velocities  $v$  such that  $mv^2/2$  is comparable to  $\Delta E_{ab}$ ; however, it is argued that these low velocities make a very small contribution to the velocity average which is weighted by  $v^3 \exp(-mv^2/2kT)$ , so that even large errors in  $S$  (e.g., factors of 2) have no effect. This argument is sufficient for calculating half-widths since one encounters only diagonal  $S$  matrix elements, and it is sufficient for inelastic transitions to states of lower energy. However, inelastic transitions to states of higher energy cannot take place *at all* unless the kinetic energy exceeds the inelastic energy increase  $\Delta E_{ab}$ . While this threshold behavior only occurs for kinetic energies  $mv^2/2 \leq E_{ab} \ll kT$ , which make a small contribution to the velocity average, the error incurred in replacing  $S_{ab} = 0$  by a finite number is quite large and results in sizable errors (10%–20%) even after the velocity average, i.e., in place of the velocity average

$$\int_0^{\infty} v^3 S\left(\frac{mv^2}{2}\right) e^{-mv^2/2kT} dv = \left(\frac{2}{m^2}\right) \int_0^{\infty} ES(E) e^{-E/kT} dE = I, \quad (21)$$

we should have

$$\begin{aligned} & \left(\frac{2}{m^2}\right) \int_{\Delta E}^{\infty} ES(E) e^{-E/kT} dE \\ &= \left(\frac{2}{m^2}\right) e^{-\Delta E/kT} \int_0^{\infty} (E + \Delta E) S(E + \Delta E) e^{-E/kT} dE \\ &\cong \left(\frac{2}{m^2}\right) e^{-\Delta E/kT} \int_0^{\infty} ES(E) e^{-E/kT} dE = e^{-\Delta E/kT} I. \quad (22) \end{aligned}$$

The latter constitutes an approximation in which we have used  $S(E + \Delta E) \cong S(E)$  and  $(E + \Delta E) \cong E$  within the integral. Based on earlier calculations,<sup>9</sup> these approximations should be good for  $\Delta E \ll kT$ ; since  $T = 300$  K corresponds to 6240 GHz, this approximation should be fairly good.

We will therefore correct Lam's line coupling coefficients  $w_{jk}$  for this effect by simply multiplying them by  $\exp(-E_{jk}/kT)$  with  $E_{jk} = E_j - E_k$ , where  $E_j$  and  $E_k$  are the energies of the multiplets in which the lines  $\nu_j$  and  $\nu_k$  are found. This is done whenever  $E_j > E_k$ ; the  $w_{jk}$  are not changed by this effect when  $E_j < E_k$  because  $w_{jk}$  contains  $S$  matrices which represent collisional transitions from the  $k$  multiplet to the  $j$  multiplet as noted in Eq. (19), where  $N'_a J'_a M'_a$  and  $N'_b J'_b M'_b$  are the initial states for the transitions described by the  $S$  matrices. With this correction, our line coupling coefficients will satisfy the correct detailed balance relation [Eq. (13)], whereas those calculated by Lam were simply symmetric ( $w_{jk} = w_{kj}$ ). This is a problem to be wary of when using a semiclassical theory to calculate inelastic rates or scattering amplitudes.

To summarize, then, our line coupling coefficients  $w_{jk}$  (modified) are obtained from those calculated by Lam, i.e.,  $w_{jk}(\text{Lam})$ , by introducing the following corrections:

$$\begin{aligned} w_{jk}(\text{modified}) &= w_{jk}(\text{Lam}) C_{\text{IOS}} C_{\text{DB}}, & E_j > E_k, \\ &= w_{jk}(\text{Lam}) C_{\text{IOS}}, & E_j < E_k, \end{aligned} \quad (23)$$

where  $C_{\text{IOS}}$  and  $C_{\text{DB}}$  represent the corrections for the

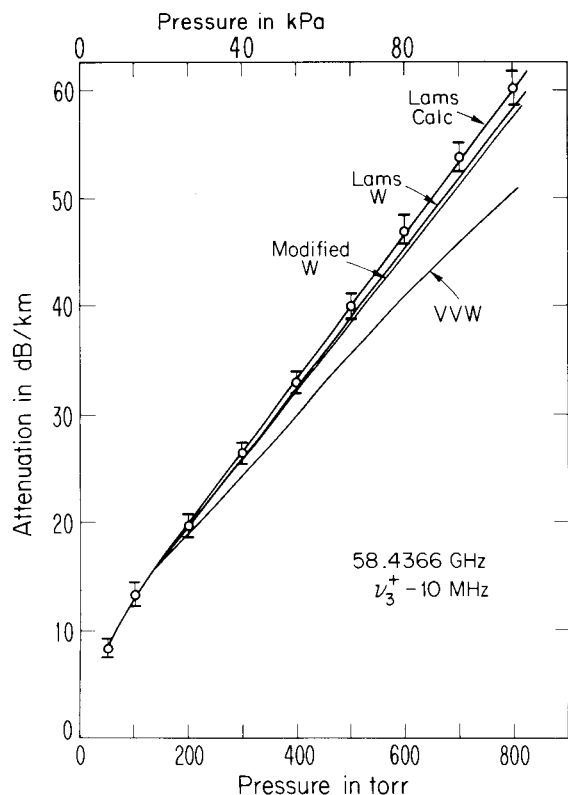


FIG. 3. Absorption at 58.4366 GHz as a function of pressure at a temperature of 300 K. Comparison of calculations with experimental data<sup>5</sup> and with Lam's calculations.<sup>3</sup>

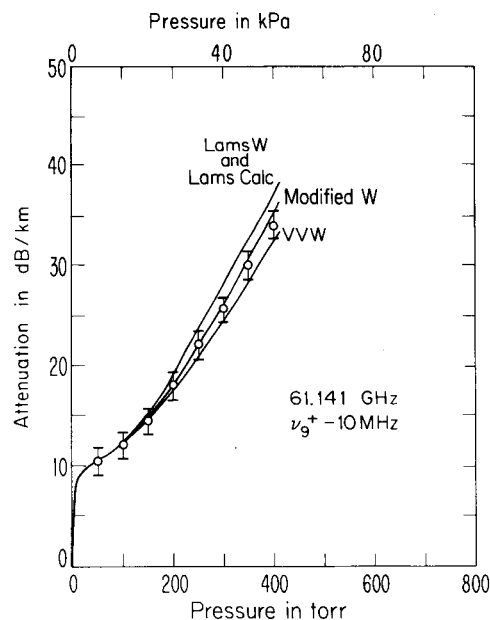


FIG. 4. Absorption at 61.141 GHz as a function of pressure at a temperature of 300 K. Comparison of calculations with experimental data<sup>5</sup> and with Lam's calculations.<sup>3</sup>

infinite order sudden approximation and detailed balance:

$$C_{\text{IOS}} = \exp\left[-(6\pi^2 E_{jk} \gamma_m / \alpha \bar{v})^{2/3} + (\epsilon + 0.5 E_{jk}) / kT\right], \quad (24)$$

$$C_{\text{DB}} = \exp[-E_{jk} / kT]. \quad (25)$$

### III. CALCULATIONS

#### A. Absorption

Our calculations employ two computer programs, one using matrix inversion and another using the perturbation theory discussed in Sec. IIC. To test the matrix inversion routine, a comparison was made with calculations of the absorption coefficient published by Lam.<sup>3</sup> For this comparison, we used the line coupling coefficients  $w_{jk}$  just as they are given in Lam's thesis.<sup>4</sup> Lam's method of calculating  $w_{jk}$  becomes somewhat time consuming and expensive for large  $N$  so he performed explicit calculations only for  $N \leq 11$  and approximated the values for  $13 \leq N \leq 33$  by various extrapolation procedures. The functional form of these extrapolations was given [Eqs. (113) and (114) of Ref. 3] but unfortunately none of the extrapolation coefficients were published. We have therefore performed a similar extrapolation for  $N > 11$  but we find that uncertainties in this extrapolation procedure can produce uncertainties in  $w_{jk}$  ranging from 10% for small  $N$  to 50% for values of  $N$  around 33. For the frequencies  $\nu_3^+$  and  $\nu_9^+$  (Figs. 3 and 4) the contribution from  $N > 11$  lines becomes important for pressures above 26 kPa (200 Torr) and for  $\nu_{21}^+$  (Fig. 5) these lines are dominant at all pressures. These uncertainties for  $N > 11$  are expected to produce some disparity between our calculations and Lam's results. In Figs. 3-5, we have plotted experimental data<sup>5</sup> together with Lam's results<sup>3</sup> and our calculations. Our results include calculations with Lam's  $w_{jk}$  coefficients denoted in the figures by "Lam's  $w$ ," calculations with the corrected

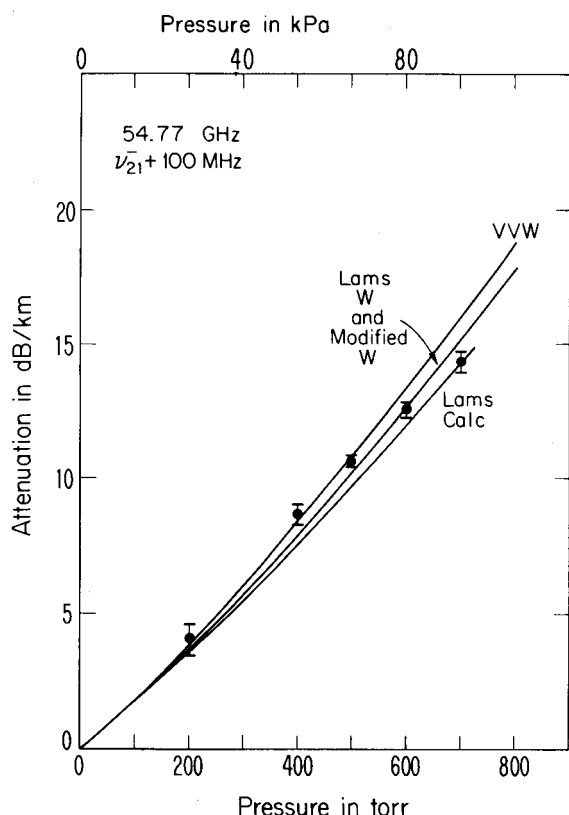


FIG. 5. Absorption at 54.77 GHz as a function of pressure at a temperature of 300 K. Comparison with experimental data<sup>5</sup> and with Lam's calculations.<sup>3</sup>

$w_{jk}$  given in Eq. (23) denoted by "modified  $w$ ," and calculations using  $w_{jk}=0$  for  $j \neq k$  denoted by "VVW" to provide a comparison with a simple Van Vleck-Weisskopf calculation and thereby illustrate the magnitude of the effect of the line coupling coefficients.

In spite of the uncertainties for  $N > 11$ , our calculations using Lam's  $w_{jk}$  agree to within 4% with the results obtained by Lam, thereby providing a check on our computer program using matrix inversion. Calculations performed with the second order perturbation theory discussed in Sec. II C' agreed with our matrix inversion calculations to better than 1% so they were not plotted. For the absorption coefficient, our perturbation calculations performed with only first order terms agreed with the second order results to better than 1% for all pressures up to 100 kPa (1 atm). This is somewhat better than one would predict for a perturbation expansion in powers of  $Pw_{jk}/\nu_{jk}$  since all such terms are about 0.1 or smaller for  $P=100$  kPa (1 atm); however, there is considerable cancellation among the higher order terms which reduces the actual error. The perturbation calculation breaks down rapidly for pressures the order of 5 atm or larger.

From Figs. 3-5 it is clear that our corrections to Lam's  $w_{jk}$  [Eqs. (21)-(23)] slightly improve the agreement with experimental data for  $\nu_9^*$  and  $\nu_{21}$  while the agreement for the  $\nu_3^*$  line is slightly worse. These changes, while observable, are not at all significant because the effect is very small and the O<sub>2</sub>-O<sub>2</sub> potential

is not known well enough to permit a serious analysis of such a small effect. One can only conclude that the influence of the line coupling coefficients is clearly observable but their effect on the absorption coefficient is too small to distinguish between the different methods of calculation.

## B. Line coupling effects in absorption and dispersion

In the previous section it was noted that, for  $P \lesssim 100$  kPa (1 atm), the absorption is not very sensitive to the line coupling coefficients. The reason for this may be seen in Eq. (17) where, to first order in pressure, the numerator is proportional to the sum  $w_{kk} + (\nu - \nu_k)y_k$ . The terms  $w_{kk}$  result in a series of simple Lorentzian profiles (a Van Vleck-Weisskopf calculation) while the "interference coefficients"  $y_k$  contain the effect of the line coupling coefficients  $w_{jk}$  [see Eq. (15)]. The half-widths  $w_{kk}$  are the order of 200 MHz/Pa (1.5-2 MHz/Torr) whereas, from Table II, we see that  $y_k$  is typically the order of 200 Pa or  $1.5 \times 10^{-4}$  Torr<sup>-1</sup>. The correction term  $(\nu - \nu_k)y_k$  is thus comparable to  $w_{kk}$  only when  $(\nu - \nu_k)$  is on the order of  $10^4$  MHz, i.e., these correction terms are important only in the far line wings where the Lorentzian has fallen off to  $10^{-8}$  of its value at the line center. It is thus not surprising that the line coupling coefficients do not have a big effect on absorption.

Dispersion, on the other hand, is extremely sensitive to the line coupling coefficients as seen from Eq. (18) in which the numerator is, to first order in pressure, proportional to  $(\nu - \nu_k) + (Pw_{kk})(Py_k)$ . The terms  $(\nu - \nu_k)$  again give the dispersion for a series of simple Lorentzian lines while  $(Pw_{kk})(Py_k)$  represents the lowest order correction due to line coupling effects. In this case the normal dispersion, proportional to  $(\nu - \nu_k)$ , vanishes at line center so the addition of the correction term  $(Pw_{kk})(Py_k)$  is very important. In fact, so much information is obtained from the dispersion calculations that it is desirable, for the sake of clarity, to discuss each frequency separately.

We note in passing that the computer programs for dispersion calculations, both by matrix inversion and perturbation theory, have been checked by detailed comparisons with the Rosenkranz results<sup>7</sup> and with those obtained by Liebe *et al.*<sup>8</sup>; the latter authors supplied a copy of their program to facilitate this comparison.

## C. Dispersion at 61.141 GHz

Our calculations of dispersion for this frequency are compared with the measurements by Liebe *et al.*<sup>5</sup> in Fig. 6. The frequency of 61.141 GHz lies 10 MHz to the red of the 9<sup>\*</sup> line; hence, the dispersion is dominated by this line for pressures below 6.7 kPa (50 Torr). The half-width for the 9<sup>\*</sup> line is 230 MHz/Pa or 1.74 MHz/Torr and  $y_{9^*} = -4.7 \times 10^{-3}$ /Pa =  $-3.5 \times 10^{-5}$ /Torr so the first order correction due to line coupling  $(Pw_{kk})(Py_k)$  will be comparable to or larger than the frequency detuning  $(\nu - \nu_k) = 10$  MHz for pressures greater than 53 kPa (400 Torr). Unfortunately, the neighboring lines also make a sizable contribution at these pressures so



TABLE II. List of half-widths  $w_{jk}$ , interference coefficients  $y_k$ , and second order coefficients  $G_k$  and  $\delta\nu_k$  for the first 20 rotational manifolds.

N	$w_{jk}$ (MHz/Torr)		$y_k$ (Torr <sup>-1</sup> )		$G_k$ (Torr <sup>-2</sup> )		$\delta\nu_k$ (MHz/Torr <sup>2</sup> )	
	Minus	Plus	Minus	Plus	Minus	Plus	Minus	Plus
1	2.14	2.21	$-7.77 \times 10^{-6}$	$+3.06 \times 10^{-4}$	$-1.24 \times 10^{-10}$	$-8.91 \times 10^{-8}$	$-6.75 \times 10^{-7}$	$2.10 \times 10^{-5}$
3	1.99	1.96	$-2.88 \times 10^{-4}$	4.50	$-5.25 \times 10^{-8}$	$-1.36 \times 10^{-7}$	$-2.71 \times 10^{-5}$	4.74
5	1.89	1.86	-2.74	3.35	-7.04	$-5.00 \times 10^{-8}$	-3.85	4.39
7	1.82	1.79	-2.34	2.15	-4.08	+3.94	-3.26	3.06
9	1.76	1.74	$-8.36 \times 10^{-5}$	$9.80 \times 10^{-6}$	+7.48	8.02	-2.16	1.86
11	1.71	1.70	+7.53	$-1.38 \times 10^{-4}$	5.66	5.69	-1.14	$8.15 \times 10^{-6}$
13	1.67	1.66	$1.921 \times 10^{-4}$	-2.31	3.67	1.16	$-5.23 \times 10^{-6}$	3.76
15	1.64	1.63	2.74	-2.95	$3.02 \times 10^{-9}$	$-8.14 \times 10^{-9}$	-2.43	1.64
17	1.60	1.60	3.31	-3.43	$-1.97 \times 10^{-8}$	$-3.23 \times 10^{-8}$	$-9.04 \times 10^{-7}$	$3.65 \times 10^{-7}$
19	1.57	1.57	3.73	-3.81	-4.09	-4.34	$+7.98 \times 10^{-10}$	-4.53
21	1.54	1.54	4.06	-4.11	-5.47	-6.26	$5.78 \times 10^{-7}$	-9.29
23	1.51	1.51	4.33	-4.31	-6.00	-6.17	$9.50 \times 10^{-7}$	$-1.13 \times 10^{-6}$
25	1.49	1.49	4.53	-4.48	-9.19	-9.05	$1.13 \times 10^{-6}$	-1.25
27	1.46	1.46	4.65	-4.59	-7.79	-7.60	1.20	-1.29
29	1.44	1.44	4.77	-4.68	$-1.02 \times 10^{-7}$	-9.87	1.22	-1.29
31	1.41	1.41	4.86	-4.75	$-8.72 \times 10^{-8}$	-8.34	1.20	-1.25
33	1.39	1.39	4.93	-4.80	$-1.09 \times 10^{-7}$	$-1.04 \times 10^{-7}$	1.16	-1.19
35	1.36	1.36	4.98	-4.84	$-9.66 \times 10^{-8}$	$-9.15 \times 10^{-8}$	1.11	-1.13
37	1.33	1.33	5.09	-4.94	$-8.52 \times 10^{-8}$	$-8.04 \times 10^{-8}$	1.21	-1.21
39	1.30	1.30	7.19	-6.95	$-1.95 \times 10^{-7}$	$-1.82 \times 10^{-7}$	$1.78 \times 10^{-5}$	$-1.72 \times 10^{-5}$

the effect of line coupling at  $(\nu - \nu_9^*) = -10$  MHz is much smaller than it would be at line center  $(\nu = \nu_9^*)$ . Nevertheless, it is easy to see from Fig. 6 that our corrections to Lam's  $w_{jk}$  are basically correct and also very important in terms of achieving agreement with the experimental data. At this frequency, the interference coefficients  $y_k$  [Eq. (15)] calculated with Lam's  $w_{jk}$  actually have the wrong sign and produce an increase in dispersion above the VVW calculation whereas the experimental data lie below the VVW curve. Our corrections to Lam's  $w_{jk}$  produce a sign change in the  $y_k$  which lowers the dispersion below the VVW curve and produces reasonably good agreement with experiment.

The reason for this rather dramatic effect, namely, the sign change, can be seen by looking at the interference coefficient  $y_{9^*}$ , which is the most important of the  $y_k$  for this frequency. From Eq. (15) we see that  $y_k$  is given by a sum of terms which, due to the  $1/\nu_{jk}$  factors, is dominated by the lines closest in frequency to  $\nu_{9^*}$ :

$$y_{9^*} \cong 2(w_{7+9^*}/\nu_{9+7^*}) + 2(w_{11+9^*}/\nu_{9+11^*}) + \dots, \quad (26)$$

where we have used  $(d_{7^*}/d_{9^*}) \cong (d_{11^*}/d_{9^*}) \cong 1$ , which is correct to about 10%. Both  $w_{7+9^*}$  and  $w_{11+9^*}$  are negative as is  $\nu_{9+11^*}$ ; hence, the first term is negative while the second is positive and they tend to cancel out one another to some extent. This cancellation is typical for all  $y_k$  because the contribution from  $\nu_j > \nu_k$  lines has a sign opposite to that for  $\nu_j < \nu_k$ . Lam's calculation gives  $w_{7+9^*} < w_{11+9^*}$  and, since  $|\nu_{9+11^*}| < \nu_{9+7^*}$ , the second term dominates and  $y_{9^*}$  is positive. Our correction for the infinite order sudden approximation [Eq. (24)] reduces both  $w_{7+9^*}$  and  $w_{11+9^*}$  slightly but our correction in Eq. (25), for the fact that upward rates such as  $w_{11+9^*}$  should be reduced by  $\exp(-\Delta E/kT)$  relative to downward rates  $w_{9+11^*}$ , reduces  $w_{11+9^*}$  whereas  $w_{7+9^*}$  is unchanged. The latter correction causes the first term to become domi-

nant and  $y_{9^*}$  is then negative.

It is thus clear that the correction for detailed balance [Eq. (25)] is extremely important due to the subtraction of upward from downward rates in the calculation of  $y_k$ ; in the case of  $y_{9^*}$  it even produces a change of sign. The

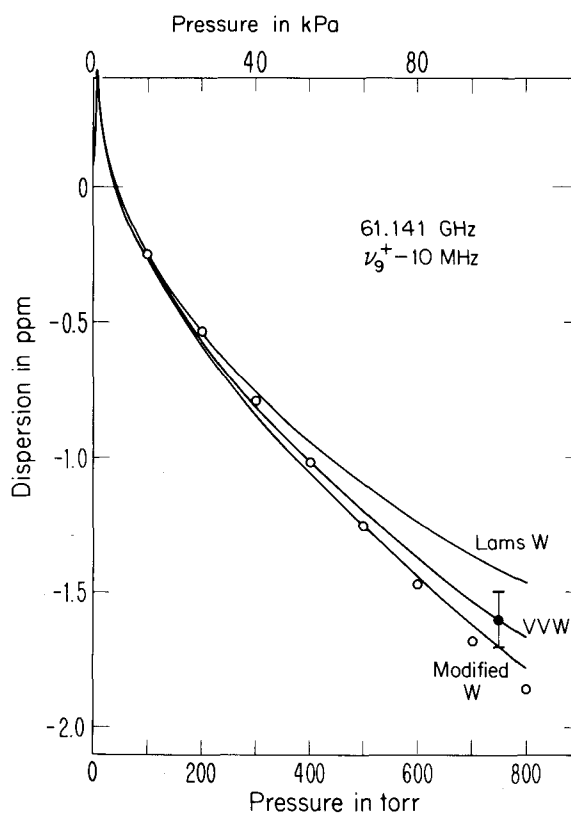


FIG. 6. Dispersion<sup>21</sup> at 61.141 GHz as a function of pressure at a temperature of 300 K. Experimental points taken from Fig. 27 of Ref. 5.

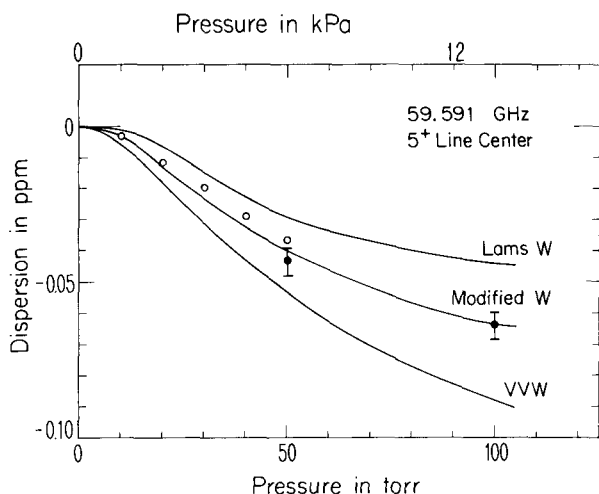


FIG. 7. Dispersion<sup>21</sup> at 59.591 GHz as a function of pressure at a temperature of 300 K. Experimental points, solid and open circles, obtained from two independent unpublished measurements.<sup>6</sup>

correction for the infinite order sudden approximation [Eq. (24)] multiplies both upward and downward rates by a factor which decreases as  $N$  decreases. This correction thus determines the size of the change due to line coupling effects. For the 9<sup>+</sup> line  $C_{10S} \cong 0.65$ ; if this correction were absent, i. e.,  $C_{10S} \cong 2.2$ , our calculations at 800 Torr would drop to about  $-2$  in Fig. 6. Such a change would be clearly observable and the agreement with experimental data would deteriorate slightly. We may thus conclude that our  $C_{10S}$  correction is also approximately correct. Finally, we note that a calculation using first order perturbation theory agrees with the full matrix inversion calculation to better than 1.5% for pressures less than 106 kPa (800 Torr).

#### D. Dispersion at 59.591 GHz

This frequency is at the center of the 5<sup>+</sup> line; hence, the dispersion due to this line, the  $k = 5^+$  term in Eq. (18), is proportional to  $P^2(\delta\nu_{5^+} + w_{5^+,5^+}y_{5^+})$ . From Table II it is clear that the second order pressure shift  $\delta\nu_{5^+}$  is negligible compared with the product  $w_{5^+,5^+}y_{5^+}$ ; thus, the dispersion due to the 5<sup>+</sup> line is directly proportional to the line coupling coefficient  $y_{5^+}$ .

For pressures below 150 Torr, the dispersion at 59.591 GHz is determined by the 5<sup>+</sup> line and by a simple VVW contribution from all neighboring lines, i. e., for  $k \neq 5^+$ ,  $(\nu - \nu_k) \gg P^2(\delta\nu_k + w_{kk}y_k)$ ; hence, the only line coupling coefficient which influences the dispersion below 27 kPa (200 Torr) is  $y_{5^+}$ . Since the VVW contribution is determined entirely by line strengths and half-widths which are known<sup>8</sup> to better than 2%, the VVW contribution can be calculated with the same accuracy and subtracted from experimental measurements to provide an essentially direct measurement of  $y_{5^+}$ .

Figure 7 shows the comparison between theory and experiment<sup>6</sup> for low pressures. The VVW contribution is again plotted separately to illustrate the effect due to line coupling coefficients. For  $P < 13$  kPa ( $P < 100$  Torr)

$y_{5^+}$  provides 99% of the contribution due to line coupling effects and at 26 kPa (200 Torr) it still represents over 75% of this effect. Thus, for  $P \leq 13$  kPa ( $P \leq 100$  Torr), the difference between the experimental data and the VVW calculation provides a direct measurement of  $y_{5^+}$ , whose accuracy is limited in this case by the  $\pm 10\%$  uncertainty in the experimental data. From this comparison it is clear that our modified  $w_{jk}$  produce a  $y_{5^+}$  coefficient which is in excellent agreement with experimental data whereas the unmodified  $w_{jk}$  as calculated by Lam produce a  $y_{5^+}$  which is a factor of 2 too large.

This analysis may be carried one step further by noting that [cf. Eq. (15)]

$$y_{5^+} \cong 2[(0.789 w_{3^+,5^+}/1144.4) - (0.853 w_{7^+,5^+}/843.8)] + \dots \\ = (w_{3^+,5^+} - 1.47 w_{7^+,5^+}) 1.379 \times 10^{-3} + \dots, \quad (27)$$

where  $w_{jk}$  is in MHz/Torr and  $y_{5^+}$  is in Torr<sup>-1</sup>. The two terms in Eq. (27) provide over 90% of the value of  $y_{5^+}$ ; the sum over the remaining lines contributes less than 10% because the terms are smaller due to the frequency differences in the denominator and the fact that contributions from  $\nu_j > \nu_{5^+}$  have signs opposite to those for  $\nu_j < \nu_{5^+}$ . This means that  $y_{5^+}$  is essentially determined by the difference in line coupling between the 5<sup>+</sup> manifold and the two neighboring manifolds. An experimental determination of  $y_{5^+}$  provides a very sensitive measurement of inelastic transition rates [recall that  $w_{jk}$  is proportional to inelastic transition amplitudes (19)].

As the pressure increases, the interference coefficients  $y_k$  for neighboring lines become important and, for  $P > 40$  kPa (300 Torr), the total effect of line coupling is greater than the VVW contribution, as shown in Fig. 8. The dispersion is very small for this frequency because it lies at the center of the 60 GHz band; see Fig. 2, where the negative contribution from lower frequency lines almost balances out the positive contribution from higher frequency lines. Due to this strong cancellation, the perturbation calculation is less accurate at this frequency, being about 8% too high at 80 kPa (600 Torr) as shown in Fig. 7 and about 15% too high at 107 kPa (800 Torr). This was the worst case for the perturbation calculation and the agreement with the experimental data<sup>6</sup> is still quite good.

#### E. Dispersion at 60.4348 GHz

This frequency lies at the center of the 7<sup>+</sup> line which is particularly interesting because it is a member of the (7<sup>+</sup>, 5<sup>-</sup>) doublet. It should be emphasized that none of the so called doublets in the 60 GHz band arise from any kind of quantum effect such as the splitting of degenerate levels, etc. They all occur simply because the frequencies of two lines happen to lie close to one another. It also happens, again by accident, that each of the four doublets (3<sup>-</sup>, 13<sup>+</sup>), (7<sup>+</sup>, 5<sup>-</sup>), (3<sup>+</sup>, 9<sup>-</sup>), and (15<sup>-</sup>, 1<sup>+</sup>) involves one line from the  $\nu_N^+$  branch and one from the  $\nu_N^-$  branch.

At first glance, it would seem that the relatively small frequency separations between the two members of a doublet would result in a correspondingly large

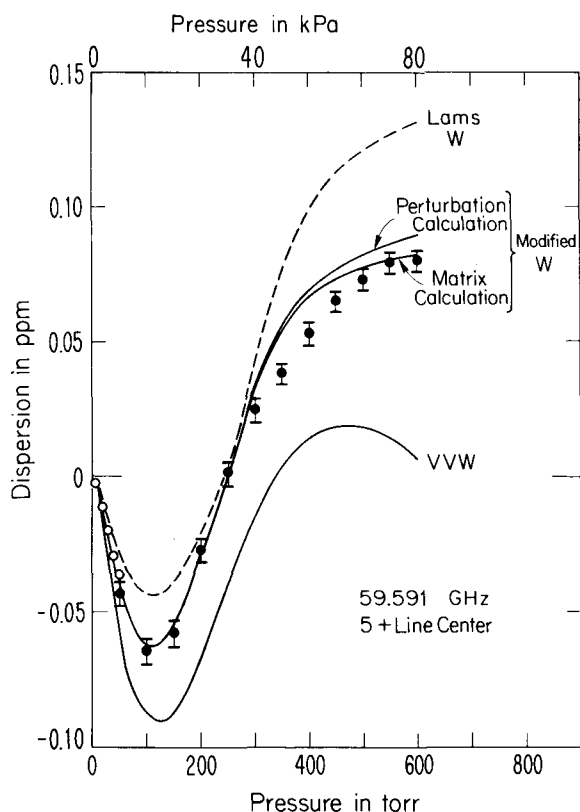


FIG. 8. Dispersion<sup>21</sup> at 59.591 GHz as a function of pressure at a temperature of 300 K. Experimental points, solid and open circles, obtained from two independent unpublished measurements.<sup>6</sup>

contribution to the interference coefficients  $y_k$ , defined in Eq. (15), because the frequency separation appears in the denominator. However, this does not happen because the line coupling coefficients  $w_{jk}$  are very small for the doublets. This occurs for two reasons; first of all, all doublets except ( $7^+$ ,  $5^-$ ) involve a rather large difference in  $N$  and the  $S$  matrix elements which couple two such levels will be very small; secondly, the coupling between the  $\nu_N^+$  and  $\nu_N^-$  branches is relatively small due to a propensity rule<sup>18</sup> whereby the  $S$  matrix elements  $\langle N, J, M | S | N', J', M' \rangle$  are reduced for  $\Delta J \neq \Delta N$ . For example,  $w_{jk}$  for  $j = \nu_N^+$ ,  $k = \nu_N^-$  is obtained from Eq. (19) by setting

$$\begin{aligned} & (N_a, J_a, N_b, J_b; N'_a, J'_a, N'_b, J'_b) \\ & = (N, N, N, N+1; N', N', N', N'-1); \end{aligned}$$

thus,  $w_{jk}$  is proportional to

$$\begin{aligned} & \langle N, N, M_a | S | N', N', M'_a \rangle \\ & \times \langle N, N+1, M_b | S | N', N'-1, M'_b \rangle^* . \end{aligned}$$

In this product the term  $\langle N, N, M_a | S | N', N', M'_a \rangle$  becomes smaller as  $\Delta N = (N - N')$  increases and  $\langle N, N+1, M_b | S | N', N'-1, M'_b \rangle$  is always small because  $\Delta J = (N+1) - (N'-1) = \Delta N + 2 \neq \Delta N$ . For these reasons, the coupling between members of a doublet has a much smaller effect on  $y_k$  than one would initially expect. In the case of interest here, the coupling between  $7^+$  and  $5^-$  accounts for 23% of the value of  $y_{7^+}$ .

In addition to the above effect on the  $y_k$ , the relatively small frequency spacing between members of a doublet is also important simply because the lines overlap at much lower pressures. This is illustrated very clearly by the dispersion at the center of the  $7^+$  line where, at 10 Torr, the  $y_{7^+}$  term in Eq. (18) contributes only 2% of the observed dispersion whereas the wing of the  $5^-$  line, i. e., the  $(\nu - \nu_{5^-})$  term in Eq. (18), provides the rest. Even at 13 kPa (100 Torr), where the  $y_{7^+}$  term is an order of magnitude larger, there is a strong overlap effect because the  $y_{5^-}$  contribution from the neighboring line is almost equal in magnitude to the  $y_{7^+}$  term but opposite in sign; the combined effect of these two terms is thus an order of magnitude smaller and again the  $(\nu - \nu_{5^-})$  contribution represents over 80% of the observed dispersion. That is why the calculations plotted in Fig. 9 show such a small change due to line coupling effects even though the frequency lies exactly at the line center. One should not be misled into thinking that the interference coefficients themselves are small simply because the experimental data<sup>6</sup> agree so closely with a simple VWV calculation. On the contrary, the interference coefficients for the  $7^+$  and  $5^-$  lines are about the same magnitude as any other  $y_k$  listed in Table II; it is simply the strong cancellation due to the overlap with the  $5^-$  line and the fact that  $y_{7^+}$  and  $y_{5^-}$  are opposite in sign that drastically reduces the effect of line coupling at this frequency.

#### F. Dispersion at 58.4366 GHz

This frequency lies 10 MHz to the red of the  $3^+$  line which is a member of the ( $3^+$ ,  $9^-$ ) doublet. For this doublet,  $w_{9^-, 3^+}$  is so small that it contributes only about 2% to the value of  $y_{3^+}$  whereas the  $w_{9^+, 3^+}$  and  $w_{1^+, 3^+}$  terms contribute 93%. In addition,  $y_{9^-}$  is less than  $0.2y_{3^+}$  so there is no appreciable cancellation from the interference term of the  $9^-$  line [recall that in the ( $7^+$ ,  $5^-$ ) doublet discussed in the previous section there was a very large cancellation effect because  $|y_{5^-}| \cong |y_{7^+}|$ ]. This means that the effect of line coupling is determined entirely by  $w_{9^+, 3^+}$  and  $w_{1^+, 3^+}$  through the  $y_{3^+}$  term

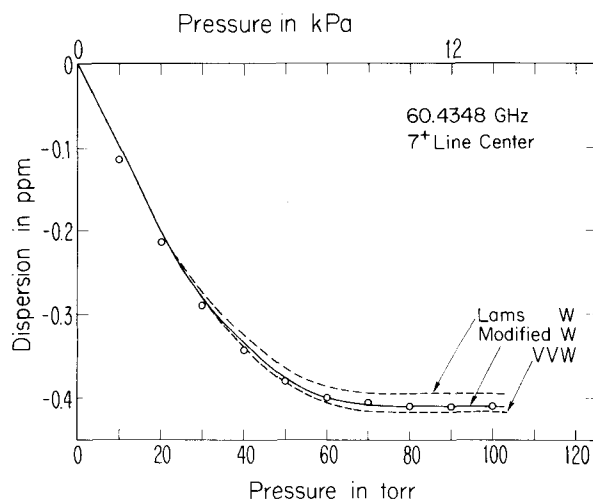


FIG. 9. Dispersion<sup>21</sup> at 60.4348 GHz as a function of pressure at a temperature of 300 K. Experimental points from Ref. 6.

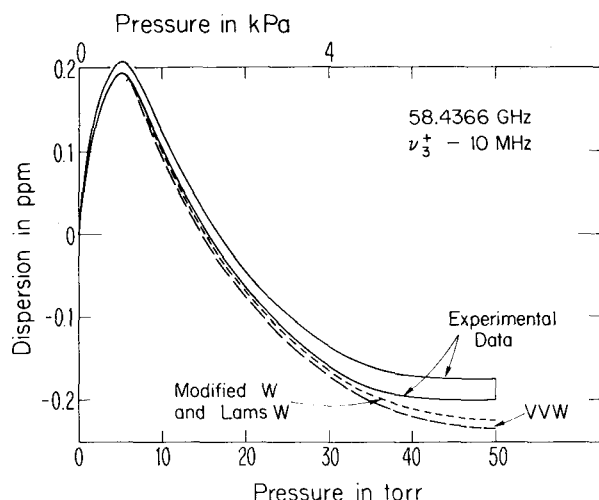


FIG. 10. Dispersion<sup>21</sup> at 58.4366 GHz as a function of pressure at a temperature of 300 K. Experimental points from Fig. 14 of Ref. 5.

for pressures below 50 Torr; for higher pressures,  $y_{3+}$  remains dominant, but, due to overlap with neighboring lines, the combined effect of the other  $y_k$  is also appreciable, contributing about 1/3 as much as  $y_{3+}$  at 107 kPa (800 Torr).

From Figs. 10 and 11 it is clear that our calculated  $y_{3+}$  does not provide very good agreement with the experimental data.<sup>5</sup> We would obtain good agreement if

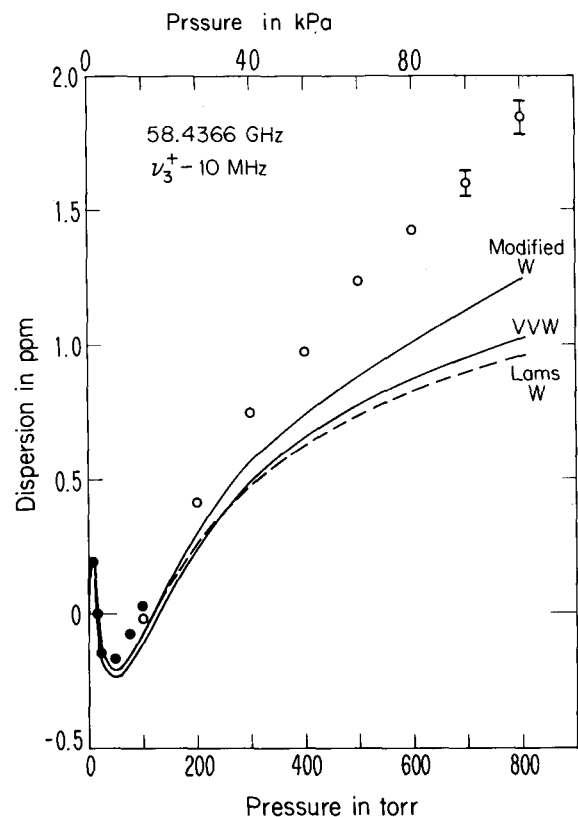


FIG. 11. Dispersion<sup>21</sup> at 58.4366 GHz as a function of pressure at a temperature of 300 K. Experimental points from Fig. 14, solid circles, and Fig. 29, open circles, of Ref. 5.

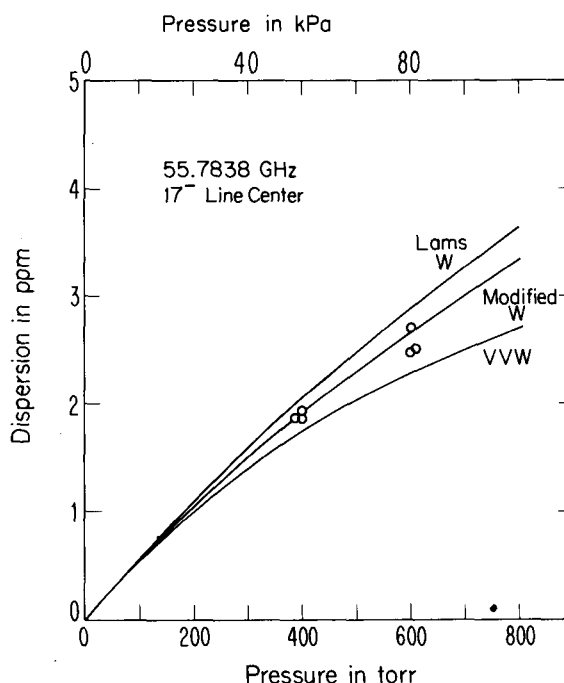


FIG. 12. Dispersion<sup>21</sup> at 55.7838 GHz as a function of pressure at a temperature of 300 K. Experimental points from Ref. 6.

our calculated  $y_{3+}$  were four or five times larger but it is hard to see how such a large change in  $y_{3+}$  could be produced by reasonable changes in our correction factors  $C_{IOS}$  and  $C_{DB}$  [Eqs. (24) and (25), respectively] or by possible additional errors in Lam's calculations of  $w_{3+,3+}$  and  $w_{3+,3+}$ . It is always possible that the experimental data are incorrect but this seems unlikely since the high pressure and low pressure data represent two different runs and both sets of data indicate that our calculations are too low. Consequently, the reason for this discrepancy is not known at the present time.

#### G. Dispersion at 55.7838, 56.9682, and 63.5685 GHz

These frequencies correspond to the centers of the 17<sup>-</sup>, 13<sup>-</sup>, and 17<sup>+</sup> lines, respectively. They are grouped together because we have experimental data<sup>6</sup> only at 400 and 600 Torr which, due to the overlapping of the lines at these pressures, is not sufficient to permit analysis of the individual  $y_k$ . These data are nonetheless interesting because they provide further confirmation of our method for correcting the line coupling coefficients calculated by Lam (see Figs. 12–14).

#### IV. CONCLUSIONS

In the present paper we have performed calculations of absorption and dispersion [defined in Eq. (3)] at various frequencies in the 60 GHz band of O<sub>2</sub> for pressures ranging from a few Torr, where the spectral lines are isolated, to 100 kPa (1 atm), where the lines have merged to form a continuous absorption band. At the higher pressures, collisions which transfer excitation from one radiating state to another, the so called line coupling transitions, are no longer effective

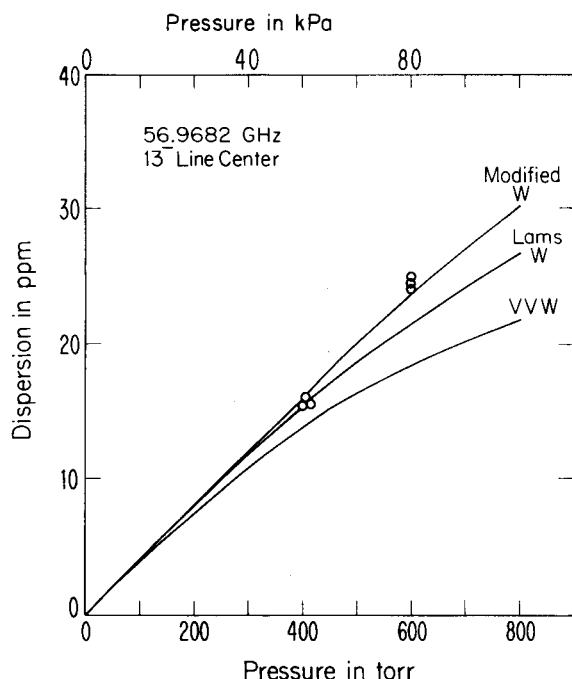


FIG. 13. Dispersion<sup>21</sup> at 569682 GHz as a function of pressure at a temperature of 300 K. Experimental points from Ref. 6.

as a broadening mechanism. The physics of this problem has been understood for some time<sup>2</sup> but a reliable quantitative calculation of the effect has been lacking because (1) a calculation of the line coupling coefficients  $w_{jk}$  was not practical with older  $S$  matrix theories and has only recently been attempted using a modern semiclassical approach,<sup>3,4</sup> and (2) a straightforward calculation of the band shape is itself very time consuming because it involves the inversion of a large matrix (about  $40 \times 40$ ) for each pressure and frequency of interest. The original motivation for the present work was to first study the validity of the perturbation technique proposed by Rosenkranz,<sup>7</sup> which reduces the time required for the matrix inversion by about two orders of magnitude, and second to perform calculations with the line coupling coefficients obtained by Lam.<sup>3,4</sup>

The perturbation approach was tested by means of comparisons between first and second order perturbation calculations and a complete matrix inversion calculation. It was found that the simple first order perturbation expressions given in Eqs. (17) and (18) are accurate to within 1% or 2% for  $P \lesssim 100$  kPa (1 atm) except for the dispersion calculations at the center of the band. At the band center the dispersion passes through zero (see Fig. 2) due to a strong cancellation in the contributions from neighboring lines. This cancellation requires that the contributions from the individual lines be calculated with very high accuracy and the perturbation theory had some difficulty here as seen in Fig. 8. Perturbation calculations for absorption seemed to be accurate to about 500 kPa (5 atm) and at that point one may be approaching the limit of validity for a binary collision theory.

The prescription used by Rosenkranz<sup>7</sup> for his calculation of the line coupling coefficients  $w_{jk}$  was based on

the fully classical model of Gordon<sup>2</sup> in which the  $w_{jk}$  were regarded as inelastic transition rates. Actually, the  $w_{jk}$  are sums over inelastic transition amplitudes (i. e.,  $S$  matrix elements) which do not satisfy a conservation of probability equation  $\sum_{jk} w_{jk} = 0$  as assumed by Gordon<sup>2</sup> and Rosenkranz.<sup>7</sup> Consequently, the Rosenkranz prescription is incorrect and provides only an order of magnitude estimate of the  $w_{jk}$ . Calculations using the Rosenkranz method for absorption and dispersion<sup>5,6,8</sup> produced results that were in fair agreement with experimental data although clear discrepancies remained and the results were extremely sensitive to the half-width for the nonresonant lines (e. g., Fig. 4 of Ref. 8), which is contrary to what one would expect. In addition, the best fit to the data required values for the nonresonant linewidth and  $w_{jk}$  coefficients which were in clear disagreement with the values calculated by Lam,<sup>4</sup> differing by factors of 2 to 5. We therefore performed absorption and dispersion calculations using the  $w_{jk}$  obtained by Lam. These calculations were not at all sensitive to the nonresonant linewidth as expected; they provided very good agreement with absorption measurements as already noted by Lam<sup>3</sup> but they gave extremely poor agreement with dispersion measurements as shown in his Figs. 3–18.

It was subsequently determined that the  $w_{jk}$  calculated by Lam are in error due to two approximations used in his theory. The first of these is the "infinite order sudden approximation" in which one neglects the energy difference between two states when calculating the inelastic transition amplitude (i. e.,  $S$  matrix) for transitions from one to the other; this approximation is known to overestimate the transition amplitude by an amount which increases with the rotational quantum number (e. g., see Ref. 16). Secondly, Lam assumed

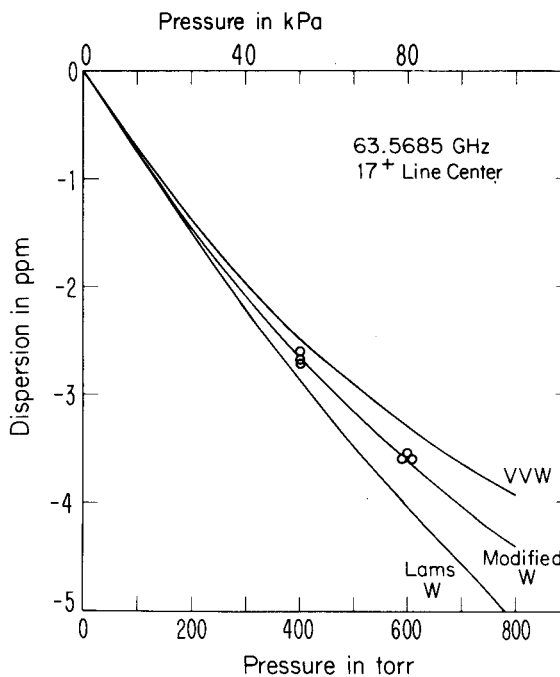


FIG. 14. Dispersion<sup>21</sup> at 63,5685 GHz as a function of pressure at a temperature of 300 K. Experimental points from Ref. 6.

that an upward inelastic transition (i. e., to a state of higher energy) can occur even in the limit of small kinetic energies when actually such a transition is forbidden for kinetic energies smaller than the energy spacing between the two states; this approximation prevents Lam's  $w_{jk}$  from satisfying the detailed balance condition [Eq. (13)]. A scheme for correcting these approximations was developed in Sec. II E and calculations with the modified  $w_{jk}$  gave generally very good agreement with all experimental data, an exception being the dispersion for the 3\* line (Figs. 10 and 11).

It may thus be concluded that absorption is not sufficiently sensitive to the line coupling coefficients to manifest the rather serious errors in the line coupling coefficients  $w_{jk}$  calculated by Lam and the Rosenkranz prescription. In the dispersion calculations, on the other hand, these errors produce very large effects, sometimes giving the wrong sign as in the case of the 9\* line discussed in Sec. III C.

Perhaps the most important result of the present work is the discovery that the dispersion is very sensitive to the line coupling coefficients. In particular, it was found that, near the line center, the low pressure data [ $P \lesssim 20$  kPa (150 Torr)] were usually governed by a single interference coefficient  $y_k$  and this in turn was determined by the difference between the line coupling coefficients  $w_{jk}$  for coupling to the two closest neighboring lines. One of these coefficients will correspond to an upward inelastic transition and thus be relatively small whereas the other will correspond to a downward transition and be somewhat larger. This means that a dispersion measurement will usually be extremely sensitive to one or two inelastic transition rates. A set of dispersion measurements for a series of spectral lines could thus provide a convenient test for calculations of state to state inelastic transition amplitudes.

To design such an experiment, one would first estimate a set of half-widths  $w_{kk}$  and interference coefficients  $y_k$  calculated by using Eq. (15) and the "rates"  $w_{jk}$  to the two nearest states. The dispersion at the center of the  $\nu_k$  line would then be given by  $(y_k/w_{kk})$  plus a series of contributions from neighboring lines [Eq. (18)]. The  $(y_k/w_{kk})$  contribution will generally be dominant if it is greater than  $(\nu - \nu_{k'}) / [(\nu - \nu_{k'})^2 + (Pw_{k'k'})^2]$  for the two neighboring lines  $k'$  but even if this is not the case, the half-widths are generally well known and this particular overlap contribution could be calculated and subtracted out. It would be preferable to avoid contributions from the interference coefficients from neighboring lines so one would want to work at pressures low enough that  $(Py_{k'})/(Pw_{k'k'}) / [(\nu - \nu_{k'})^2 + (Pw_{k'k'})^2]$  is always less than  $(y_k/w_{kk})$ . In this manner it should be possible to design a set of experiments which would measure a set of interference coefficients  $y_k$  and thereby provide a good test for calculated inelastic transition amplitudes.

It should be mentioned that the corrected line coupling coefficients calculated in this paper are subject to errors resulting from the approximate nature of the correction terms in Eqs. (24) and (25) as well as additional errors

in Lam's  $w_{jk}$  due to uncertainties in the intermolecular potential.

## APPENDIX

In this Appendix we will derive our perturbation expansion for the eigenvalues  $\Lambda_k$  and eigenvectors  $|\chi_k\rangle$  of the operator  $\nu_0 + iPW$  introduced in Eq. (4). We will use a very simple perturbation method (e.g., Merzbacher,<sup>19</sup> Wilkinson<sup>20</sup>) which is slightly complicated by the subspace of zero eigenvalues (i. e., the nonresonant lines). The subspace corresponding to zero eigenvalues will be called  $\Omega_0$  and the rest of the space will be  $\Omega_1$  so that the notation  $j \in \Omega_0$  implies  $\nu_j = 0$  and  $j \in \Omega_1$  means  $\nu_j \neq 0$ . At this point it is convenient to define a set of vectors  $|\phi_j\rangle$  which are orthogonal normalized linear combinations of  $|j\rangle \in \Omega_0$  defined by

$$\langle \phi_j | w | \phi_k \rangle = \delta_{jk} w_{kk}, \quad (\text{A1})$$

i. e., the vectors  $|\phi_j\rangle$  are the eigenvectors of the part of  $w$  which exists in  $\Omega_0$ .

The perturbation expansions for  $|\chi_k\rangle$  and  $\Lambda_k$  are defined by

$$|\chi_k\rangle = |\chi_k^{(0)}\rangle + P|\chi_k^{(1)}\rangle + P^2|\chi_k^{(2)}\rangle + \dots, \quad (\text{A2})$$

$$\Lambda_k = \Lambda_k^{(0)} + P\Lambda_k^{(1)} + P^2\Lambda_k^{(2)} + \dots, \quad (\text{A3})$$

where  $|\chi_k^{(n)}\rangle$  and  $\Lambda_k^{(n)}$  are the  $n$ th order perturbations and it is required that  $\langle \chi_k^{(0)} | \chi_k^{(n)} \rangle = 0$  for  $n \neq 0$ . Substituting Eqs. (A2) and (A3) into

$$(\nu_0 + iPw)|\chi_k\rangle = \Lambda_k|\chi_k\rangle \quad (\text{A4})$$

and equating like powers of  $P$  produces the set of equations

$$\nu_0|\chi_k^{(0)}\rangle = \Lambda_k^{(0)}|\chi_k^{(0)}\rangle, \quad (\text{A5})$$

$$(\nu_0 - \Lambda_k^{(0)})|\chi_k^{(1)}\rangle = -iw|\chi_k^{(0)}\rangle + \Lambda_k^{(1)}|\chi_k^{(0)}\rangle, \quad (\text{A6})$$

$$(\nu_0 - \Lambda_k^{(0)})|\chi_k^{(2)}\rangle = -iw|\chi_k^{(1)}\rangle + \Lambda_k^{(1)}|\chi_k^{(1)}\rangle + \Lambda_k^{(2)}|\chi_k^{(0)}\rangle, \quad (\text{A7})$$

which are then solved for  $|\chi_k^{(n)}\rangle$  and  $\Lambda_k^{(n)}$ . The zeroth order equation [Eq. (A5)] is readily solved by (recall that  $\nu_0|\phi_k\rangle = 0$  since  $|\phi_k\rangle$  is a linear combination of  $|j\rangle \in \Omega_0$ )

$$\Lambda_k^{(0)} = \nu_k \quad (\text{all } k), \quad (\text{A8})$$

$$|\chi_k^{(0)}\rangle = |k\rangle \quad (k \in \Omega_1), \\ = |\phi_k\rangle \quad (k \in \Omega_0). \quad (\text{A9})$$

The first order equation [Eq. (A6)] may be multiplied from the left by  $\langle k|$  if  $k \in \Omega_1$ , or by  $\langle \phi_k|$  if  $k \in \Omega_0$ , to yield [using Eqs. (A5), (A8), and (A9)]

$$\Lambda_k^{(1)} = i\langle k|w|k\rangle \quad (k \in \Omega_1), \\ = i\langle \phi_k|w|\phi_k\rangle \quad (k \in \Omega_0). \quad (\text{A10})$$

For  $k \in \Omega_1$ , we obtain the components of  $|\chi_k^{(1)}\rangle$  by multiplying Eq. (A6) from the left by  $\langle j| \in \Omega_1$  and  $\langle \phi_j|$  using the notation  $\nu_{jk} = \nu_j - \nu_k$  to obtain

$$|\chi_k^{(1)}\rangle = -i \sum_{j \neq k} |j\rangle \frac{\langle j|w|k\rangle}{\nu_{jk}} + i \sum_{j \in \Omega_0} |\phi_j\rangle \frac{\langle \phi_j|w|k\rangle}{\nu_k} \quad (k \in \Omega_1). \quad (\text{A11})$$

For  $k \in \Omega_0$ , we can determine the components of  $|\chi_k^{(1)}\rangle$  in  $\Omega_1$  by multiplying Eq. (A6) with  $\langle j| \in \Omega_1$  but we cannot determine  $\langle \phi_j|\chi_k^{(1)}\rangle$  or  $\langle j|\chi_k^{(1)}\rangle$  for  $j, k \in \Omega_0$  because  $(\nu_0 - \nu_k)$  vanishes. We therefore write

$$|\chi_k^{(1)}\rangle = -i \sum_{j \in \Omega_1} |j\rangle \frac{\langle j|w|\phi_k\rangle}{\nu_j} + \sum_{j \neq k} |\phi_j\rangle \alpha_{jk} \quad (k \in \Omega_0), \quad (\text{A12})$$

where the  $\alpha_{jk}$  will be determined by the next higher order equation. In Eqs. (A11) and (A12) we were careful

to sum over  $j \neq k$  so that  $\langle \chi_k^{(0)}|\chi_k^{(1)}\rangle = 0$ ; in fact, the condition  $\langle \chi_k^{(0)}|\chi_k^{(n)}\rangle = 0$  for  $n \neq 0$  is a general requirement for this type of perturbation theory.

Proceeding to the second order equation [Eq. (A7)], we again multiply by  $\langle k|$  if  $k \in \Omega_1$  or by  $\langle \phi_k|$  if  $k \in \Omega_0$  and obtain

$$\Lambda_k^{(2)} = \sum_{j \neq k} \frac{\langle k|w|j\rangle \langle j|w|k\rangle}{\nu_{jk}} - \sum_{k \in \Omega_0} \frac{\langle k|w|\phi_j\rangle \langle \phi_j|w|k\rangle}{\nu_k} \quad (k \in \Omega_1),$$

$$= \sum_{j \in \Omega_1} \frac{\langle \phi_k|w|j\rangle \langle j|w|\phi_k\rangle}{\nu_j} \quad (k \in \Omega_0). \quad (\text{A13})$$

We again determine the components of  $|\chi_k^{(2)}\rangle$  for  $k \in \Omega_1$  by multiplying Eq. (A7) with  $\langle j| \in \Omega_1$  and  $\langle \phi_j| \in \Omega_0$ :

$$|\chi_k^{(2)}\rangle = \sum_{j \neq k} |j\rangle \left( \frac{\langle j|w|k\rangle \langle k|w|k\rangle}{\nu_{jk}^2} - \sum_{l \neq k} \frac{\langle j|w|l\rangle \langle l|w|k\rangle}{\nu_{jk} \nu_{lk}} + \sum_{l \in \Omega_0} \frac{\langle j|w|\phi_l\rangle \langle \phi_l|w|k\rangle}{\nu_{jk} \nu_k} \right) + \sum_{j \in \Omega_0} |\phi_j\rangle \left( \frac{\langle \phi_j|w|k\rangle \langle k|w|k\rangle}{\nu_k^2} + \sum_{l \in \Omega_1} \frac{\langle \phi_j|w|l\rangle \langle l|w|k\rangle}{\nu_k \nu_{lk}} - \sum_{l \neq j} \frac{\langle \phi_j|w|\phi_l\rangle \langle \phi_l|w|k\rangle}{\nu_k^2} \right) \quad (k \in \Omega_1). \quad (\text{A14})$$

For  $k \in \Omega_0$ , multiplying Eq. (A7) by  $\langle \phi_j|$  provides an expression for the coefficients  $\alpha_{jk}$  introduced in Eq. (A12):

$$\alpha_{jk} = i \sum_{l \in \Omega_1} \frac{\langle \phi_j|w|l\rangle \langle l|w|k\rangle}{\nu_l (\langle \phi_j|w|\phi_j\rangle - \langle \phi_k|w|\phi_k\rangle)}, \quad (\text{A15})$$

and multiplying Eq. (A7) by  $\langle j| \in \Omega_1$  provides

$$|\chi_k^{(2)}\rangle = \sum_{j \in \Omega_1} |j\rangle \left( \frac{\langle j|w|k\rangle \langle \phi_k|w|\phi_k\rangle}{\nu_j^2} - \sum_{l \in \Omega_1} \frac{\langle j|w|l\rangle \langle l|w|k\rangle}{\nu_j \nu_l} \right) + \sum_{j \in \Omega_0} |\phi_j\rangle \beta_{jk}, \quad (\text{A16})$$

where again the coefficients  $\beta_{jk}$  would be determined by the next higher order equation.

At this point it is desirable to make some simplifying approximations regarding the nonresonant lines. We first note that for  $j, k \in \Omega_0$ , the diagonal matrix elements  $\langle k|w|k\rangle$  are at least one order of magnitude greater<sup>4</sup> than the off diagonal elements  $\langle j|w|k\rangle$ . A vector  $|\phi_k\rangle$  will thus equal  $|k\rangle$  plus a small admixture (10% or less) of other  $\Omega_0$  states. Since the nonresonant lines contribute at most 10% to the dispersion and less than 1% to absorption in the vicinity of the 60 GHz lines, we will use  $|\phi_k\rangle \cong |k\rangle$  with a probable error of at most 1%. Our next approximation is to neglect the coefficients  $\alpha_{jk}$  defined in Eq. (A15). This coefficient appears only in Eq. (A12) where it represents the first order correction to the wave function  $|\chi_k\rangle$  within the  $\Omega_0$  subspace. Using the  $w$  matrix elements calculated by Lam (which overestimate  $\alpha_{jk}$ ), the maximum value of  $\alpha_{jk}$  is about 0.1/atm; thus, even at a pressure of 1 atm,  $\alpha_{jk}$  represents only a 10% correction to  $|\chi_k\rangle$  with-

in the  $\Omega_0$  subspace; neglecting  $\alpha_{jk}$  thus represents about a 1% error in dispersion and 0.1% in absorption for the 60 GHz lines. Finally, we neglect the terms  $\beta_{jk}$  introduced in Eq. (A16) for the same reasons.

With the above approximations, our results may be written in the form

$$\Lambda_k = \nu_k + iP \langle k|w|k\rangle + P^2 \sum_{j \neq k} \langle k|w|j\rangle \langle j|w|k\rangle / \nu_{jk} + \dots, \quad (\text{A17})$$

$$|\chi_k\rangle = |k\rangle - iP \sum_{j \neq k} |j\rangle \langle j|w|k\rangle / \nu_{jk} + P^2 \sum_{j \neq k} |j\rangle \langle j|w|k\rangle \langle k|w|k\rangle / \nu_{jk}^2 - P^2 \sum_{j \neq k} \sum_{l \neq k} |j\rangle \langle j|w|l\rangle \langle l|w|k\rangle / \nu_{jk} \nu_{lk} + \dots, \quad (\text{A18})$$

which are valid for all  $k$  provided that we interpret  $\sum_{j \neq k}$  as  $\sum_{j \in \Omega_1}$  whenever  $k \in \Omega_0$ . In order to normalize  $|\chi_k\rangle$ , we divide by the square root of (recall that  $\langle \chi_k^{(0)}|\chi_k^{(n)}\rangle = 0$  for  $n \neq 0$ )

$$\langle \chi_k|\chi_k\rangle = 1 + \langle \chi_k^{(1)}|\chi_k^{(1)}\rangle + \dots = 1 - \sum_{j \neq k} \langle k|w|j\rangle \langle j|w|k\rangle / \nu_{jk}^2 + \dots \quad (\text{A19})$$

It should be noted that  $\langle \chi_k|$  is the transpose<sup>20</sup> of  $|\chi_k\rangle$ , not the Hermitian adjoint (the matrix  $\nu_0 + iPw$  is not Hermitian). The transformation matrix  $X_{jk}$  whose columns are the normalized  $|\chi_k\rangle$  eigenvectors is thus given by

$$\begin{aligned}
X_{jk} &= \langle j | \chi_k \rangle / \sqrt{\langle \chi_k | \chi_k \rangle} \\
&\cong \delta_{jk} \left( 1 + \frac{1}{2} P^2 \sum_{i \neq k} w_{ki} w_{ik} / \nu_{ik}^2 \right) + (1 - \delta_{jk}) (-i P w_{jk} / \nu_{jk} \\
&\quad + P^2 w_{jk} w_{kk} / \nu_{jk}^2 - P^2 \sum_{i \neq k} w_{ji} w_{ik} / \nu_{jk} \nu_{ik}) + \dots,
\end{aligned}
\tag{A20}$$

$$\begin{aligned}
(X^{-1})_{kj} &= \langle \chi_k | j \rangle / \sqrt{\langle \chi_k | \chi_k \rangle} \\
&= \delta_{kj} \left( 1 + \frac{1}{2} P^2 \sum_{i \neq k} w_{ki} w_{ik} / \nu_{ik}^2 \right) + (1 - \delta_{jk}) (-i P w_{kj} / \nu_{jk} \\
&\quad + P^2 w_{kj} w_{kk} / \nu_{jk}^2 - P^2 \sum_{i \neq k} w_{ki} w_{ij} / \nu_{jk} \nu_{ik}) + \dots.
\end{aligned}
\tag{A21}$$

It is easy to verify by matrix multiplication that  $\sum_j (X^{-1})_{ij} X_{jk} = \delta_{ik} + O(P^3)$  and that  $\sum_{jm} (X^{-1})_{ij} \langle j | (\nu_0 + i P w) | m \rangle \chi_{mk} = \Lambda_k \delta_{ki} + O(P^3)$ .

<sup>1</sup>E. W. Smith, M. Giraud, and J. Cooper, *J. Chem. Phys.* **65**, 1256 (1976).

<sup>2</sup>R. G. Gordon, *J. Chem. Phys.* **46**, 448 (1967).

<sup>3</sup>K. S. Lam, *J. Quant. Spectrosc. Radiat. Transfer* **17**, 351 (1977).

<sup>4</sup>K. S. Lam, Ph.D. Thesis, Dept. Of Physics, University of California, Berkeley, January 1976.

<sup>5</sup>H. J. Liebe, Dept. of Commerce, Office of Telecommunications Report 76-65, June 1975.

<sup>6</sup>G. Gimmestad and H. J. Liebe (unpublished data).

<sup>7</sup>P. W. Rosenkranz, *IEEE Trans. Antennas Propag.* **23**, 498 (1975).

<sup>8</sup>H. J. Liebe, G. G. Gimmestad, and J. D. Hopponen, *IEEE Trans. Antennas Propag.* **25**, 327 (1977).

<sup>9</sup>E. W. Smith and M. Giraud, *J. Chem. Phys.* **71**, 4209 (1979).

<sup>10</sup>M. Baranger, *Phys. Rev.* **111**, 494 (1958); **112**, 855 (1958).

<sup>11</sup>E. W. Boom, D. Frenkel, and J. van der Elsken, *J. Chem. Phys.* **66**, 1826 (1977).

<sup>12</sup>Using Lams<sup>3</sup> Eq. (34) and the fact that  $k(\nu)$  and  $n(\nu) - 1$  are the real and imaginary parts of an analytic function, see for example, R. Loudon, *The Quantum Theory of Light* (Clarendon, Oxford, 1973), Chaps. 2 and 4.

<sup>13</sup>A. Ben Reuven, *Phys. Rev.* **145**, 7 (1966).

<sup>14</sup>J. H. Van Vleck, *Phys. Rev.* **71**, 413 (1947).

<sup>15</sup>T. A. Dillon and J. T. Godfrey, *Phys. Rev. A* **5**, 599 (1972).

<sup>16</sup>R. Goldflam, S. Green, and D. J. Kouri, *J. Chem. Phys.* **67**, 4149 (1977).

<sup>17</sup>H. S. W. Massey, *Electronic and Ionic Impact Phenomince* (Clarendon, Oxford, 1971), Vol. III, Chap. 17.4, particularly Eqs. (133) and (166).

<sup>18</sup>For the O<sub>2</sub> molecule, the spin S is very weakly coupled to the nuclear angular momentum N to form the resultant J. Therefore, a collision which produces a sudden change in N will tend to leave S unchanged, resulting in  $\Delta S = 0$  or  $\Delta J = \Delta N$ . This is not a rigorous selection rule because S will be able to follow N for slow adiabatic collisions; hence, we observe only a propensity for  $\Delta J = \Delta N$  collisions, i. e., the S matrix elements for  $\Delta J \neq \Delta N$  are small but not zero.

<sup>19</sup>E. Merzbacher, *Quantum Mechanics* (Wiley, New York, 1961), Chap. 16.

<sup>20</sup>J. H. Wilkinson, *The Algebraic Eigenvalue Problem* (Clarendon, Oxford, 1965), pp. 1-7 and 66-70.

<sup>21</sup>In Figs. 6-14 we have actually plotted  $\Delta N(\nu) - \Delta N(\nu/2)$ , where  $\Delta N$  is the dispersion function defined in Eq. (3) and  $\nu$  is the observation frequency, e. g.,  $\nu = 61.141$  GHz in Fig. 6. The experimental apparatus of Liebe *et al.*<sup>5,6,8</sup> is designed to measure this function rather than  $\Delta N(\nu)$  itself in order to subtract out the frequency independent refractivity.